Hawai'ian coral holobionts reveal algal and prokaryotic host specificity, intraspecific variability in bleaching resistance, and common interspecific microbial consortia modulating thermal stress responses

Laura Núñez-Pons[1,2]*, Ross Cunning[3], Craig Nelson[4], Anthony Amend[5], Emilia M. Sogin[6], Ruth Gates[7], Raphael Ritson-Williams[8]

1 Department of Integrative Marine Ecology (EMI), Stazione Zoologica Anton Dohrn, Villa Comunale, 80121 Napoli, Italy

2 NBFC, National Biodiversity Future Center, Palermo 90133, Italy

3 Daniel P. Haerther Center for Conservation and Research, John G. Shedd Aquarium, 1200 South Lake Shore Drive, Chicago, IL 60605, USA.

4 Sea Grant College Program, University of Hawai'i at Mānoa, Honolulu, HI, USA

5 Pacific Biosciences Research Center, University of Hawai'i at Mānoa, Honolulu, HI 96822, USA

6 Molecular and Cell Biology, University of California Merced, Merced, CA, USA

7 Hawai'i Institute of Marine Biology, University of Hawai'i at Mānoa, Honolulu, HI, USA

8 College of Arts and Sciences, The Heart of Santa Clara University, Vari Hall 500 El Camino Real Santa Clara, CA 95053, USA

*Corresponding author: laura.nunezpons@szn.it

Contributing authors: rcunning@sheddaquarium.org, craig.nelson@hawaii.edu, amend@hawaii.edu, esogin@ucmerced.edu, rgates@hawaii.edu, rritson-williams@calacademy.org

Abstract

Historically, Hawai'i had few massive coral bleaching events, until two consecutive heatwaves in 2014–2015. Consequent mortality and thermal stress were observed in Kane'ohe Bay (O'ahu). The two most dominant local species exhibited a phenotypic dichotomy of either bleaching resistance or susceptibility (*Montipora capitata* and *Porites compressa*), while the third predominant species (*Pocillopora acuta*) was broadly susceptible to bleaching. In order to survey shifts in coral microbiomes during bleaching and recovery, 50 colonies were tagged and periodically monitored. Metabarcoding of three genetic markers (16S rRNA gene ITS1 and ITS2) followed by compositional approaches for community structure analysis, differential abundance and correlations for longitudinal data were used to temporally compare Bacteria/Archaea, Fungi and Symbiodiniaceae dynamics. *P. compressa* corals recovered faster than *P. acuta* and *Montipora capitata*. Prokaryotic and algal communities were majorly shaped by host species, and had no apparent pattern of temporal acclimatization. Symbiodiniaceae signatures were identified at the colony scale, and were often related to bleaching susceptibility. Bacterial compositions were practically constant between bleaching phenotypes, and more diverse in *P. acuta* and *M. capitata*. *P. compressa*'s prokaryotic community was dominated by a single bacterium. Compositional approaches (via microbial balances) allowed the identification of fine-scale differences in the abundance of a consortium of microbes, driving changes by bleaching susceptibility and time across all hosts. The three major coral reef founder-species in Kane'ohe Bay revealed different phenotypic and microbiome responses after 2014–2015 heatwaves. It is difficult to forecast, a more successful strategy towards future scenarios of global warming. Differentially abundant microbial taxa across time and/or bleaching susceptibility were broadly shared among all hosts, suggesting that locally, the same microbes may modulate stress responses in sympatric coral species. Our study highlights the potential of investigating microbial balances to identify fine-scale microbiome changes, serving as local diagnostic tools of coral reef fitness.

Keywords

Coral microbiome, thermal bleaching, compositional analysis, microbial balances, Symbiodiniaceae ITS2 profiles.

1. Introduction

Microbial symbioses play critical roles in the ecology and evolution of corals (Ainsworth et al., 2020; Bourne et al., 2016). The majority of research on microbial communities in corals has focused on single celled dinoflagellates in the family Symbiodiniaceae (zooxanthellae), since these symbionts play a large role in coral health and nutrition (Baker, 2003; Sampayo et al., 2008; D'Angelo, 2015). Less studied are the populations of Bacteria, Archaea and even Fungi that associate with corals forming the coral holobiont (Bourne et al., 2016). As seawater temperatures increase, coral bleaching is occurring more frequently around the world, which is a stress-induced disruption of symbiosis between the host and symbiotic algae, causing a "bleached" pale-to-white appearance of affected colonies (Douglas 2003). Bleached corals, depleted of symbiotic algae (Fitt et al., 2001; Jokiel 2004; Falkowski et al., 1984) may effectively starve until the symbiosis is reestablished (Baker 2001). Resistance and recovery following bleaching are highly variable both among and within coral species, and may be influenced by environmental factors (e.g., light, temperature, symbiont availability), as well as traits of the host and its associated microbial communities (Edmunds 1994; Fitt et al., 2001; Baird et al., 2009; Grottoli et al., 2014; Conti-Jerpe et al., 2020; Ainsworth and Gates, 2016). Additionally, the coral animal may be able to switch to heterotrophy to mitigate starvation, and recover faster due to the accumulation of lipids (Grottoli et al., 2006; Hughes and Grottoli 2013; Wall et al., 2019; Conti-Jerpe et al., 2020); while genetic and epigenetic processes may also promote stress resilience (Edmunds 1994; Fitt et al., 2001; Grottoli et al., 2014; Baird et al., 2009; Putnam and Gates 2015).

The diversity of Symbiodiniaceae in relation to coral bleaching has been researched for over 30 years (Rowan and Powers 1991; van Oppen and Medina 2020), as different genotypes have different physiological responses to abiotic conditions (Baker 2003; Sampayo et al., 2008). For instance, there are thermally tolerant symbionts (e.g., *Cladocopium thermophilum, Durusdinium glynnii, D. trenchii*) that increase bleaching resistance of coral hosts (Baker 2001;

Berkelmans and van Oppen 2006, Sampayo et al., 2008; Fisher et al., 2012; Hume et al., 2015; Silverstein et al., 2015). The majority of coral species associate with a single species of Symbiodiniaceae (LaJeunesse et al., 2018; Howells et al., 2020), but some are capable of hosting multiple species and/or genera within one coral colony (Rowan et al., 1997; Baker 2003; Gardner et al., 2019; Hume et al., 2019, 2020). These two strategies are illustrated in three dominant sympatric corals found in Hawai'i, with *Porites compressa* only presenting *Cladocopium* C15, *Pocillopora acuta* combining *C. pacificum/C. latusorum* (C1d/C42), and *Montipora capitata* hosting either *Cladocopium* C31or *Durusdinium glynnii*, or both simultaneously in the same colonies (LaJuenesse et al., 2004; Innis et al., 2018; Stat et al., 2013; Turnham et al., 2021). There is some evidence of symbiont shuffling in some coral species (Baker 2001, Cunning et al., 2015), but this may occur rarely or not at all in others, as reported in *Pocillopora* spp. (McGinley et al., 2012) and *M. capitata* (Cunning et al., 2016). This inflexibility could be intrinsic of those holobionts, or due to the particular conditions of disturbance and recovery not favoring Symbiodiniaceae rearrangements.

Beyond Symbiodiniaceae, patterns of symbiosis with microorganisms forming the coral holobiont are less understood (Amend et al., 2012; Ainsworth and Gates, 2016; Boilard et al., 2020). The coral prokaryotic microbiome is thought to have a core component (Ainsworth et al., 2015; Hernandez-Agreda et al., 2017), as well as a set of unique microbes (Hernandez-Agreda et al., 2018), and rare dynamic taxa that can vary in individuals even within species (Epstein et al., 2019). Stability in coral microbial associations may be beneficial or deleterious, depending on the context (Ainsworth and Gates, 2016). Community shifts involving increases in opportunistic, potentially pathogenic taxa and decreases in beneficial taxa, have been observed during induced and natural bleaching stress (Bourne et al., 2005; Littman et al., 2011); including studies on *P. compressa* (Vega Thurber et al., 2009) and *Pocillopora* (Tout et al., 2015). Other work has shown that microbial stability may either promote thermal tolerance (Ziegler et al., 2017; Epstein et al., 2019; Gardner et al., 2019), and/or hamper acclimatization, with deleterious effects on the host (Pogoreutz et al., 2018). As with Symbiodiniaceae, prokaryotic associates

may include taxa able to confer stress tolerance to the holobiont (van Oppen and Medina 2020; Ainsworth et al., 2020).

In 2014 and 2015, there were repeated massive bleaching episodes in the Hawaiian archipelago (Ritson-Williams and Gates 2020). These thermal stress events prompted us to survey the fate of coral microbiomes (Symbiodininaceae, Archaea/Bacteria, Fungi) over time during and after the heatwaves in the field. In Kane‘ohe Bay, Oahu, both *Montipora capitata* and *Porites compressa* had bleaching susceptible *vs* bleaching resistant phenotypes, while only bleaching susceptible colonies of *P. acuta* were observed. All these three dominant species were monitored and sampled throughout a year. There has been extensive research on these coral species in Hawaii (e.g., Putnam and Gates 2015; Cunning et al., 2016; Wall et al., 2019; Matsuda et al., 2020; Ritson-Williams and Gates 2020; Innis et al., 2018), however, there is little information about their associated microbiota (e.g., Salerno et al., 2011; Shore-Maggio et al., 2015; Epstein et al., 2019). This study quantifies temporal dynamics in coral microbiomes using amplicon sequencing of multiple gene regions for multiple microbial compartments, coupled with compositional data analysis, to track symbiont shifts in multiple bleaching phenotypes within and among coral species. We further inspect for microbial sentinels within the coral holobionts able to diagnose fluctuations from healthy to distressed/diseased states.

2. Materials and Methods

2.1. Study site and sampling

Consecutive coral bleaching events occurred in Hawai’i during the late summers of 2014 and 2015 (Ritson-Williams and Gates 2020). The present study focused on corals from Reef 25 in the central portion of Kane‘ohe Bay, O’ahu Island (N 21.461, W 157.823). In October 2014, 20 colonies of *Montipora capitata* (Mcap) and 20 *Porites compressa* (Pcom)

were tagged as adjacent pairs (ten totally bleached and ten non-bleached –fully dark brown, hereinafter referred to as "B" and "NB" colonies respectively for each species); along with ten colonies of fully bleached *Pocillopora acuta* (Pacu, there were no individuals of *P. acuta* that did not bleach). All tagged colonies came from 4–5 m depth, and were 50 in total (n = 10 for each sample group: Mcap_B, Mcap_NB, Pcom_B, Pcom_NB, and Pacu _B). One coral fragment (1.5 cm long) was repeatedly sub-sampled from every tagged coral on five occasions: M0 = Month 0 – October (24^{th}) 2014; M1 = Month 1 – November (24^{th}) 2014; M3 = Month 3 – January (14^{th}) 2015; M6 = Month 6 – May (6^{th}) 2015; and M12 = Month 12 – September (15^{th}) 2015, yielding a total of 250 coral fragments (Fig. 1). Covariates used in downstream analyses are given in Table S1. Coral fragments (~ 1 cm^3) were collected at each time point by snorkelers, placed in individual sterile bags and snap-frozen in liquid N within 1 minute of collection. All fragments were maintained at -80 ºC until processed.

2.2. DNA extraction, library preparation, and sequencing

DNA from coral fragments was extracted using PowerSoil® DNA Isolation Kit (Mo Bio Laboratories) following manufacturer's instructions. Amplicon sequencing of ribosomal RNA (rRNA) target gene markers for three microbial sets: Bacteria/Archaea (16S), Fungi Internal Transcribed Spacer 1 (ITS1) and Symbiodiniaceae (ITS2) was performed in three separate multiplexed runs. Due to technical issues, DNA samples from month M12 (Sept 2015) could not be sequenced for the ITS2 marker. Illumina protocol was applied with a two-PCR approach and two dual-index strategy (Caporaso et al., 2012; Kozich et al., 2013). Primer sets used were: bacterial/archaeal specific primers for V_4 region (*Escherichia coli* position: 515–806) of the small-subunit ribosomal RNA (16S) gene (515F –GTGYCAGCMGCCGCGGTAA Parada et al., 2016 and 806R –GGACTACNVGGGTWTCTAAT Apprill et al., 2015); ITS-DinoF (GTGAATTGCAGA ACTCCGTG) and ITS2rev2 (CCTCCGCTTACTTATATGCTT (Franklin et al., 2012) targeting the ITS2 for Symbiodiniaceae library; and fungi-specific primers ITS1F (CTTGGTCATTTAGAGGAAGTAA;Gardes and Bruns, 1993) and ITS2R-CoralBetter (GTGARCCAAGAGATCCRTT; designed in the present study) for ITS1.

Amplifications were performed in 25 µl reactions with NEBNext® Q5® Hot Start HiFi PCR Master Mix (New England Biolabs, Inc.), 0.8 µl BSA (Bovine Serum Albumin; 20 mg/ml), 1µl of each 5 µM primer, and 1.5µl of template. Reactions were under the thermocycling profile: 98 ºC for 2 min, then 28 cycles of 98 ºC for 15 s, 53 ºC for 30 s, 72 ºC for 30 s, final extension at 72 ºC for 2 min. The second Index PCR to attach dual indexes and Illumina sequencing adapters used forward primers with the 5'-3' Illumina i5 adapter (AATGATACGGCGACCACCGA GATCTACAC), an 8–10bp barcode and a primer pad; and reverse fusion primers with 5'-3' Illumina i7 adapter (CAAGCAGAAGACGGCATACGAGAT), an 8–10 bp barcode, a primer pad. Reactions were made in 25 µl with 0.5 µl of each 5 µM primer, and 1µl of corresponding products from first amplicon PCR reactions diluted (1:30), and with a temperature regime of: 98 ºC for 2 min, then 28 cycles of 98 ºC for 15 s, 55 ºC for 30 s, 72 ºC for 30 s, final extension at 72 ºC for 2 min. The PCR products were purified and pooled equimolar on Just-a-Plate ™ 96 PCR Purification and Normalization Kit plates following manufacturer's instructions (Charm Biotec). Paired-end sequencing was performed on an Illumina MiSeq sequencer 2 x 300 flow cell at 10 pM at Core Lab, Hawai'i Institute of marine Biology (USA).

2.3. Bioinformatics analysis

2.3.1 Sequence processing for 16 S V_4 and ITS1 sets

Fastq files containing demultiplexed 16S–V_4 and ITS1paired-end reads were imported into QIIME2 v.2020.11 (Bolyen et al., 2019). DADA2 (Callahan et al., 2016) was used for "denoising" 16S data in paired-end mode. The ITS1 region was first extracted using ITSxpress (Rivers et al., 2018). Only forward reads as in Pauvert et al., (2019) were denoised in single-end mode with DADA2 (Callahan et al., 2016), and filtered from non fungal ITS sequences (Tables S2A and S2B). Taxonomic annotation was performed using a pre-trained Naïve Bayes classifier (sklearn (Bokulich et al., 2018a, 2018c) against SILVA reference (99% identity) database v.128 (Quast et al., 2013; Yilmaz et al., 2014) trimmed to span the V_4 region (291 bp) for the 16S data. While for the ITS1 set, UNITE reference database (v. 1.12.2017) was customized adding

outgroup metazoan sequences from NCBI to check for host co-amplification (as in McGee et al., 2019; Supplementary Material S1).

2.3.2. Sequence processing for ITS2 set

Demultiplexed paired-end reads from the ITS2 Symbiodiniaceae marker were submitted to SymPortal (SymPortal.org; Hume et al., 2019) to obtain ITS2 type profile predictions, reflecting the "defining intragenomic [sequence] variants" (DIVs) in order of their relative abundance. Absolute abundance counts tables for ITS2 type profiles and underlying ITS2 sequences were formatted and imported into QIIME2 v.2020.11 (Bolyen et al., 2019) for downstream analyses (Supplementary Material S1; and Table S2C).

2.3.3. Microbial community analysis

16S ASVs and ITS2 sequence compositions were analyzed using DEICODE (https://library.qiime2.org/plugins/deicode/19/) diversity method based on Aitchison distances and robust principal component analysis (RPCA) for compositional data (Aitchison 1982; Martino et al. 2019). Standard diversity distance metrics that do not account for compositionality of data were also computed on QIIME2 v.2020.11 (Bolyen et al., 2019). Statistics were calculated using q2-diversity adonis for multi-factor permutational multivariate analysis of variance (PERMANOVA). The most informative formula in the model for the 16S data was "Species*TimePoint+Bleaching", while "Species*Bleaching" was the most explicative for ITS2. Pairwise comparisons for single covariates were run with q2-beta-group-significance. In all cases permutations were set to 999, and tests corrections significance to q value > 0.05 (i.e., FDR adjusted p value; Supplementary Material S1).

2.3.4. Longitudinal, differential abundance and co-occurrence cross networks analyses

By simultaneously analyzing our samples across all time points, meaningful signals may be lost at a particular time point. Also, having more than one measurement per subject in temporal/longitudinal or paired samples experiments violates independency assumptions

between samples of Kruskal-Wallis tests. Therefore, pairwise PERMANOVA comparisons were run for each timepoint by species. Further pertinent methods for differential abundance (Morton et al. 2019; Fedarko et al. 2020), longitudinal analyses –including pairwise differences/distances, linear-mixed-effects (LME) (Bokulich et al. 2018b), and co-occurrence cross network analyses that take into account repeated measurements and data compositionality (Shaffer 2020; Shannon et al., 2003) were performed as described in Supplementary Material S1.

R (RStudio) was applied for additional statistics and plotting (http://www.r-project.org).

3. Results

3.1 Bacteria/Archaea composition based on 16S rRNA gene data

3.1.1 Alpha and beta diversity

Pacu and Mcap corals reported higher bacterial diversity, richness and evenness (Shannon, Observed and Pielou's evenness) indexes compared to Pcom (Fig. 2, Fig. S3.1; Kruskal–Wallis H=137.94, $p < 0.001$, $p = 5.56$ e-18). Alpha diversity did not yield significant differences within species between B *vs* NB colonies in Mcap and Pcom, or across time points in any species (Tables S4; Supplementary Material S2 and S3).

Differences in beta diversity were found by Species, reporting different microbial communities in the three host species, and in the interaction Species*TimePoint; while Mcap and Pacu were more diverse from Pcom for all metrics (PERMANOVA 999 permutations, significance set to $p < 0.05$; Tables S5). Since Bacterial composition was mostly determined by host species, according to all alpha and beta diversity indexes, downstream analyses were performed within species, to test for changes over time in all three species, and between bleached and non-bleached colonies in Mcap and Pcom. Based on Aitchison distances, bacterial

composition varied in Mcap NB between M12 and M0, and from M12 with respect to the other months according to Jaccard (Supplementary Material S2 and S3; Tables S6, S7). No significant longitudinal trend was found in beta diversity across nor between timepoints in any B *vs* NB corals (Tables S6, S7, Supplementary Material S2 and S3).

3.1.2 Bacterial/Archaeal community compositions

A total of 1257 ASVs were distributed in 979 Mcap, 523 Pcom, and 737 Pacu associated taxa. Taxonomy annotation at the genus level yielded 331, 211 and 279 bacterial and archaeal genera; this was out of a total of 93, 99 and 40 coral colony fragments belonging to Mcap, Pcom and Pacu respectively. In Mcap corals a bacterial strain within order Myxococcales made up > 50% relative abundance in 35 % of the samples. Other dominant genera were *Acinetobacter* –with preponderance of *A. calcoaceticus*, and *Endozoicomonas*. The least diverse bacterial communities were found in Pcom, predominantly composed of *Endozoicomonas*. A single phylotype in this genus accounted for > 90% in relative abundance in 65 % of Pcom samples. Other representative taxa were *Acinetobacter, Candidatus Amoebophylus,* and order Myxococcales. Pacu was dominated by Proteobacteria, with one strain covering > 50% relative abundance in 43 % of the samples. Most contributing genera included *Acinetobacter* (chiefly *A. calcoaceticus*) and *Candidatus Amoebophylus*, and there was a large proportion of unclassified taxa. In variable abundances, *Pseudomonas, Bacillus, Staphylococcus, Synechococcus, Lawsonella* and unidentified strains in Myxococcales were found in all three species. While, *Micrococcus*, *Corynebacteria, Turicella, Cyanobium, Brevundimonas, Maritimonas, Aerococcus* and *Geobacillus* were more linked to Mcap and Pdam (Fig. 2; Supplementary Material S2 and S3). All coral species shared 237 taxa (19 %), with Mcap sharing more taxa with Pacu (542; 43 %), than with Pcom (395; 31 %), and Pcom and Pacu sharing the least proportion of phylotypes (282; 22 %). The largest number of unique taxa was recorded in Mcap (279), followed by Pacu (149) and Pcom (83).

3.1.3. Phylotype-wise differential abundance analysis of 16S rRNA gene data

The importance (i.e., fold change) of each ASV in relation to the covariates TimePoint (month after bleaching, M0–M12) and Bleaching susceptibility (B *vs* NB) was calculated in separate analyses within species to create microbial balances.

In Mcap the most informative balance defining longitudinal changes in B vs NB microbiomes consisted of fifteen ASVs in genera: *Endozoicomonas, Acinetobacter, Pseudomonas* in the numerator; and *Micrococcus, Synechococcus, Staphylococcus, Lawsonella, Bacillus* and order Myxococcales, in the denominator (91 out of 93 samples retained). In M0 and M6 NB colonies (ranked to numerator taxa) exhibited significantly higher log-ratios than B (associated to denominator phylotypes; Welch's tests, $p < 0.05$). In M1 and M3, NB had lower log-ratios than B colonies, but the differences were not significant. In M1 and M3, *Bacillus* was not detected as differential taxa, and *Synechoccocus* lost relevance in M6 (Material S4, Tables S8). Longitudinally, for this microbial balance, Mcap_B had higher log-ratio rankings in M3 compared with M6 and M12; whereas Mcap_NB displayed lower log-ratios in all time points with respect to M0 (LME; $p < 0.05$; Fig. 3).

Differentially abundant taxa in the balance of Pcom comprised two *Endozoicomonas* strains in the numerator, along with fluctuating taxa in *Candidatus Amoebophilus, Acinetobacter calcoaceticus, Pseudomonas stutzeri, Synechococcus, Roseitalea*; over *Staphylococcus*, *Micrococcus,* Neisseriaceae and five *Endozoicomonas* in the denominator (Material S4, Tables S8). Pcom_B corals revealed higher log-ratios in M1, with respect to Pcom_NB (Welch's tests, $p < 0.05$; Material S4, Tables S8). Longitudinally, Pcom_B displayed higher log-ratios in M1 in comparison to M0 and M6 (LME; $p < 0.05$), instead Pcom_NB showed stability across time points (LME; $p > 0.05$; Fig. 3, Material S4, Tables S8). Further longitudinal analyses can be found in Supplementary Material S2.

The most discriminative microbial balance of Pacu comprised fifteen taxa assigned to: *Endozoicomonas, Cyanobium, Acinetobacter, Pseudomonas, Neisseriaceae* in the numerator; and *Micrococcus, Lawsonella, Synechococcus, Bacillus*, *Staphylococcus* in the denominator (39 out of 40 samples kept). M0 colonies had lower log-ratios with respect to all the other time points (LME; $p < 0.05$; Tables S8; Fig. 3).

The longitudinal behavior (over time) of bacterial genera represented in the above microbial balances for the three host species were inspected in trajectory plots using centered log ratio (CLR) abundances. The investigated genera included: *Endozoicomonas, Acinetobacter, Bacillus, Candidatus Amoebophilus*, *Cyanobium*, *Lawsonella, Micrococcus, Pseudomonas, Staphylococcus, Synechococcus* and *Roseitalea*. Phylotypes included in the differential balances appertaining to family Neisseriaceae and order Myxococcales, but not assigned to genus level, were not included in this analysis (see Fig. 3, and Supplementary Material S2 for detailed interpretations).

3.2. Fungi composition based on ITS1 data

Untargeted host co-amplification was a major constraint in characterizing fungal communities, despite the new primer designed to bypass metazoan DNA. We found 94.8 % coral co-amplification, retrieving only 5.2 % overall fungal sequences. The rate of co-amplification varied among species, with *P. compressa* displaying the largest untargeted co-amplification (98.4 %), followed by *M. capitata* (95.6 %), and *P. acuta* (56 %) (Supplementary Material S2). The most represented fungal species retrieved were *Malassezia restricta, M. globosa, Hortaea_werneckii, Aspergillus penicillioides, Phellinus gilvus*. No further statistical analysis was performed due to insufficient/uneven diversity coverage.

3.3. Symbiodiniaceae composition based on ITS2 data

3.3.1. Symbiodiniaceae ITS2 type profiles

ITS2 type profiles were 29 in total, 27 belonging to the genus *Cladocopium* and 2 to *Durusdinium*. Their associations with corals depended on host species, bleaching susceptibility, and their interaction (PERMANOVA 999 permutations, $p < 0.05$). Certain coral colonies were stable over time in Symbiodiniaceae composition, but others experienced temporal shifts

without a clear pattern (Tables S9). *Cladocopium* profiles were dominant in the three host species. Only one type profile was shared between Mcap and Pacu (C1d), the rest (95 %) were only found in single host species. Mcap had the most varied profiling –10 *Cladocopium*, 2 *Durusdinium*, and were the only corals harboring *Durusdinium* types. Pcom and Pacu reported 10 and 7 distinct unshared *Cladocopium* profiles respectively (Fig. 4). The resistant phenotypes Mcap_NB reported 9 *Cladocopium* and 2 *Durusdinium* profiles, as compared to Mcap_B with 5 and 1 respectively. *Durusdinium* profiles always occurred mixed with *Cladocopium* in 4–5 Mcap_NB colonies per time point. Pcom_B displayed more assorted type profiles across individuals within each time point than Pcom_NB. Mcap_B corals acquired more varied ITS2 profiling with time –including a *Durusdinium* profile acquired in one Mcap_B colony in M6, but this effect was not statistically supported. With the exception of one sample in Mcap_B and one in Pcom_N both in M6, the presence of mixed ITS2 type profiles was only ascertained in Mcap_NB colonies with an incidence of 48% (Fig. 4).

3.3.2. Underlying Symbiodiniaceae ITS2 sequence composition

Our corals contained 173 *Cladocopium* and 28 *Durusdinium* ITS2 sequences (≥1% abundance). By coral species and bleaching susceptibility the number of different *Cladocopium* / *Durusdinium* sequences was higher in NB colonies in Mcap (Mcap_B 51 / 20 *vs* Mcap_NB 80 / 28), as opposed to Pcom that showed more sequence variability in B (Pcom_B 82 / 3 *vs* Pcom_NB 62 / 3); while Pacu reported 19 / 5.

Within the same coral species, ITS2 profiles shared common major sequences (predominant DIVs within type profiles), and were distinguished by other major and minor sequences (nonmajor DIVs, Fig. 4). Across different host species, ITS2 profiles did not share major sequences. Major *Cladocopium* DIVs designating profiles in *M. capitata* were C31 and C17d, in *P. compressa* C15, and in *P. acuta* C1d. *Durusdinium* major DIVs were D4 and D1, followed by D6, only represented as major sequences in *M. capitata*. Variations in ITS2 profiles within the same colonies across time points were therefore due to the loss, gain or substitution of minor sequences prompting a shift in profile assignment (Fig. 4).

ITS2 sequence compositions confirmed the observed pattern of ITS2 profiles, highly structured by host species and bleaching susceptibility, with no consistent temporal shifts. In the RPCA biplots Mcap showed differences in B *vs* NB colonies at M0, M1 and M3, being D1, D4 and D6 the most correlated DIVs with NB. Pcom revealed dissimilarity between B *vs* NB colonies at M0, and here D6, C15cc, C3, 70890_C and C3dg were major drivers of NB clustering, versus C15id and 70894_C associated to B (Fig. 5 and PERMANOVA 999 permutations, $p < 0.05$, Tables S10, S11, S12; Supplementary Material S2 and S3).

3.3.3. Phylotype-wise differential abundance analysis of ITS2 data

Selection of the 43% most differentially abundant ITS2 sequences in relation to covariates TimePoint (M0–M12) and Bleaching susceptibility (B *vs* NB) in *M. capitata* yielded 23 numerator and 23 denominator phylotypes (keeping 90.78 % samples). This balance discriminated Mcap_B with higher log-ratios from Mcap_NB corals in all time points. Numerator DIVs associated to Mcap_B included some C31, a few C17, C21 and other *Cladocopium* DIVs; denominator DIVs correlated to Mcap_NB comprised 55 % *Durusdinium* DIVs (D4, D1, D6, D1ab, D3h) along with a few C17 and C21 among other *Cladocopium* DIVs (Fig. 5; Tables S13).

In *P. compressa*, the top 25 % differential ITS2 sequences (maintaining 91.25 % samples) resulted in 12 phylotypes (C3 and other *Cladocopium* DIVs) in the numerator correlated Pcom_B colonies, and 12 denominator phylotypes (several C15 and other *Cladocopium* DIVs) associated to Pcom_NB in M0 and M1. In M3 and M6, when corals recovered colouration, Pcom_B and Pcom_NB corals recorded similar log-ratios (Fig. 5; Tables S13).

In *P. acuta* the model with the co-variate “TimePoint” was uninformative with respect to the null model (adding “1” in the formula), indicating no response of Symbiodiniaceae across time.

Log-ratios in the balances of differentially abundant ITS2 sequences tracked longitudinally over time had no significant shifts in any species (LME; $P<[z] < 0.05$; Supplementary Material S5, Tables S13).

3.4. Cross networks between 16S rRNA gene ASVs and ITS2 profiles

Co-occurrence cross networks illustrated potential interaction patterns among bacteria and Symbiodiniaceae, allowing to detect changes in coral microbiomes' structure. In Mcap_B a simple network in M0 formed by two C31 *Cladocopium* ITS2 profiles and few bacteria, increased conspicuously in bacterial nodes from M1 to M6, together with the addition of another C31 and a *Durusdinium* D4/D1 nodes in M3 and M6. Mcap_NB started with a complex network composed by four C31, two C17d/C31 and two D4/D1 profiles connected with dense agglomerations of bacteria. The network became less complex in M1 and M3, with the exclusion of two C31 profiles; and acquired more bacterial nodes again over M6, with the re-inclusion of C31 nodes and exclusion of a C17d/C31 node. Pcom_B started with three C15 profiles connected to few bacteria. Bacterial nodes increased over M1 with the addition of a C15 profile, and declined in M6 with the removal of a C15 node. Pcom_NB networks maintained three C15 profiles and few bacteria nodes over M0–M3. In M6 a C1d profile was added, but bacterial nodes and edges diminished. Network complexity increased in Pacu_B from M0–M1, with the increase of C1d profiles from three to four nodes, and with a progressive increment of bacterial nodes over M1–M6. Co-occurrence interconnections were predominant over co-exclusion, except in Mcap_B at M1 and Pacu_B at M3. Networks in susceptible-B colonies in the three species displayed increased positive interactions during bleaching recovery. Whereas, in resistant-NB corals the number of interactions decreased in Mcap_NB, or fluctuated in Pcom_NB. Consistently, Pcom_B and Pcom_NB maintained smaller networks (fewer nodes and edges) than the rest, with the punctual exception of Mcap_B in M0 (Fig. 6; Supplementary Material S2 for detailed results).

4. Discussion

Historically, massive coral bleaching in Hawaiian ecosystems was unusual, until 1996 (Bahr et al., 2015). The consecutive heatwaves of 2014 and 2015 in Kane‘ohe Bay allowed us to track temporal shifts in bleaching susceptible and resistant coral microbiomes *in situ*, during and after the bleaching peaks. Pcom_B corals recovered faster (after ~2.5 months) than Pacu_B (~3 months), and Mcap_B (~6 months), according to color scores (Ritson-Williams and Gates 2020), yet actual Symbiodineaceae densities could have been regained faster (Cunning et al., 2016). Prokaryotes, in turn, were expected to exhibit more rapid responses to stressors, due to their fast generation times (Ziegler et al., 2017; Glasl et al., 2017; Pogoreutz et al., 2018).

Algal and prokaryotic communities in our corals followed a species-specific pattern, frequent in sympatric populations (Gardner et al., 2019; Howells et al., 2020), whereas intraspecific Symbiodiniaceae signatures were identified at the colony scale (Rouzé et al., 2019). Mcap had the most variable ITS2 profiling, followed by Pcom and Pacu, whilst Symbiodiniaceae composition was influenced by bleaching susceptibility. Algal-genotypes conferring different bleaching resistance in conspecific hosts may appertain to the same genus, as in Pcom (Sampayo et al., 2008), or to different ones as in Mcap (Berkelmans and van Oppen 2006; Gardner et al., 2019). But also, susceptibility can be independent from symbiont-type (Smith et al., 2017; Howells et al., 2020).

Bacterial compositions were more diverse in Mcap and Pacu than in Pcom, and were practically constant between bleaching phenotypes. Microbial stability after natural thermal disturbance has been reported in corals undergoing sub-bleaching (Epstein et al., 2019) and bleaching (Gardner et al., 2019). While, community shifts were documented after induced stress (Bourne et al., 2005; Vega Thurber et al., 2009; Littman et al., 2011; Ziegler et al., 2016). In our corals, certain bacterial-ASVs/ Symbiodiniaceae-DIVs were differentially abundant across time and/or bleaching susceptibility, highlighting the potential of fine-scale microbiome changes in coral resilience (Glasl et al., 2017; Ziegler et al., 2019; Epstein et al., 2019). Below we discuss

441 the dynamics of coral microbiomes during the process of bleaching and recovery in the different
442 host species.
443
444 ***4.1. Pocillopora acuta***
445 Pacu had the highest bleaching incidence, and was associated with eight fluctuating
446 Symbiodiniaceae C1d-profiles. This agreed with the C1d-dominance described for this species
447 in Hawai'i (LaJeunesse et al., 2004). Predicted profiles dominated by C1d and C42.2 likely
448 reflect the preponderance of mixed *Cladocopium pacificum* and *C. latusorum* (Turnham et al.,
449 2021). Lack of acclimatization patterns agrees with stabilities of dominant symbionts in
450 pocilloporids under thermal stress. Whilst, profile shifting driven by minor ITS2-sequences
451 shifts, is presumably matching with background genotype variability reported in previous
452 studies (Stat et al., 2009; McGinley et al., 2012; Epstein et al., 2019). In other geographies,
453 higher bleaching thresholds have been reported in populations harboring *Durusdinium glynnii*
454 (previously D1) (Glynn et al., 2001; Wham et al., 2017; Brener-Raffalli et al., 2018; Li et al.,
455 2021; Zhou et al., 2021), or in chunky (versus fine) morphotypes, even when presenting C1d
456 (Smith et al., 2017; Epstein et al., 2019). Therefore, the bleaching incidence observed in Pacu
457 could rely on a combination of having fine morphology and *Cladocopium*–profiles, both
458 correlated to higher susceptibilities (Smith et al., 2017).
459 Bacterial communities were dominated by phylum Proteobacteria, followed by
460 Bacteroidetes, Actinobacteria, Firmicutes and Cyanobacteria, similar to pocilloporids from
461 other regions; whereas, Family Amoebophilaceae (mostly *Candidatus Amoebophylus*) and
462 genus *Acinetobacter* (largely *A. calcoaceticus*) were more preeminent, and *Endozoicomonas*
463 less abundant in Pacu (Bourne and Munn 2005; Tout et al., 2015; Brener-Raffalli et al., 2018; Li
464 et al., 2021; Zhou et al., 2021, but see Epstein et al., 2019; Osman et al., 2020). Prokaryotic
465 community, in terms of overall alpha and beta diversity, did not show significant changes over
466 time, as in other surveys involving coral bleaching (Pogoreutz et al., 2018; Gardner et al.,
467 2019). Nonetheless, microbial rearrangements could be detected via balances of differentially
468 abundant taxa, revealing lower log-ratios in corals at the bleaching peak M0. Upon recovery

(M1–M12) Pacu was correlated to *Endozoicomonas, Cyanobium*, *Acinetobacter, Pseudomonas* and *Neisseriaceae*, whereas bleached colonies in M0 were associated to *Micrococcus, Lawsonella, Synechococcus, Bacillus* and *Staphylococcus*. Likewise, cross co-occurrence networks showed an increase in node complexity and positive interconnections from M1. This implied that sparse interactions between bacteria and Symbiodiniaceae during thermal stress, increased in number as algal cells repopulated in the recovery process after M0, yielding larger networks.

Recovery in Pacu happened after 2–3 months (Ritson-Williams and Gates 2020); probably thanks to heterotrophic feeding (Lyndby et al., 2020; Dobson et al., 2021) and, microbiome rearrangements in early recovery phases (Santos et al., 2014; Ziegler et al., 2017).

4.2. Montipora capitata

Mcap colonies were associated with *Cladocopium* and *Durusdinium* symbionts. At the DIV level C31, C17 and C21 were predominant genotypes in both B and NB corals, while D4, D1, D6, D1ab and D3h characterized NB colonies, in agreement with recent studies (Matsuda 2021). Bleaching resistant Mcap_NB colonies contained either pure C or mixed D/C profiles (50 % of the times), and were different from susceptible Mcap_B, which contained basically C-profiles. Adjacent colonies never shared the same ITS2-profile. In both bleaching phenotypes, six colonies (66 %) maintained their corresponding dominant profiles, the remaining (three) experienced temporal shifts, in agreement with Cunning et al. (2016). C31-C17d-C31.1-C31a-C21-C31f-C17e-C31l-C21ac might represent a thermosensitive ITS2-profile, as 8 out of 9 Mcap_B bleached colonies in M0 contained this profile, whilst its presence in Mcap_NB (1–2 colonies) was always in combination with D-profiles. In purity or mixed, D-genotypes provide thermal resistance in *M. capitata*, but colonies with C-profiling also demonstrated stress-tolerance (Cunning et al., 2016). Our analyses based on ITS2-types (Hume et al., 2019) identified different *Cladocopium* profiles, in comparison to previous surveys reporting solely C31-genotype (LaJeunesse et al., 2004; Stat et al., 2013; Cunning et al., 2016), which could resolve the disparate stress-resistance of Mcap_NB *vs* Mcap_B. In one exception though, two

colonies containing the same profile (C31/C17d-C21-C31.9-C21ac-C17e-C31h-C31i) at M0, one underwent bleaching and the other one not, suggesting multiple factors (including different microenvironments affecting these corals) other than symbiont type regulating thermal tolerance. Mcap_B and Mcap_NB maintained different Symbiodiniaceae compositions, based on profiles and underlying ITS2-sequences, while colony heterogeneity in bleached Mcap_B increased with time, with no clear stabilization pattern. Actually, only one colony acquired a partial *Durusdinium* profile at M6, supporting the low prevalence of symbiont shuffling described in this species (Cunning et al., 2016).

Prokaryotic communities were dominated by Proteobacteria (Family P3OB-24, Order Myxococcales), and by genera *Acinetobacter* (largely *A. calcoaceticus*) and *Endozoicomonas*. In general, they matched with *M. capitata* microbiomes, characterized by the presence of Cyanobacteria and Deinococcus-Thermus, and low abundance of *Vibrio* (Shore-Maggio et al., 2015; Beurmann et al., 2018). Even if non statistically significant, increased alpha diversities observed in Mcap_B at M1 and M3 may suggest microbial rearrangements after thermal-stress (Vega Thurber et al., 2009; Tout et al., 2015; McDevitt-Irwin et al., 2017), or seasonal fluctuations in Mcap_NB at M6 (Cunning et al., 2016). Log-ratio rankings of differentially abundant taxa were higher in Mcap_NB with respect to Mcap_B at M0 and M6. At these two time points of symbiont depletion: bleaching peak (M0) and seasonal algal downturn (M6; as in Cunning et al., 2016), Mcap_NB was ranked to numerator taxa –*Endozoicomonas, Acinetobacter and Pseudomonas*; whereas bleached Mcap_B were correlated to denominator taxa –Myxococcales, *Lawsonella, Micrococcus, Synechococcus, Bacillus* and *Staphylococcus*. Cross networks became more complex in Mcap_B from M1 to M6, as algal densities recovered (M1–M3), and bacteria established interactions with Symbiodiniaceae. Instead, Mcap_NB showed higher network complexity in M0 compared to bleached Mcap_B colonies, reflecting stress response rearrangements between thermo-tolerant algal and prokaryotic symbionts during the heatwave.

M. capitata was found to rely on heterotrophy to compensate for energy losses when experimentally bleached (Grottoli et al., 2006). Mcap did not evidence such trophic plasticity,

525 and would have regained symbiont populations at expense of biomass resources by January
526 2015 (Wall et al., 2019; Ritson-Williams and Gates 2020), in agreement with the microbial
527 outcomes.
528
529 ***4.3. Porites compressa***
530 ITS2-profiling in Pcom revealed C15-dominance, in accordance with older surveys on
531 *Porites compressa* (LaJeunesse et al., 2004). Pcom_NB and Pcom_B corals held distinct
532 Symbiodiniaceae patterns 70–90 % of the times, across M0–M12. While, other characteristics
533 in the holobiont or microenvironmental variabilities causing different stress conditions, should
534 explain why 20 % adjacent Pcom_B and Pcom_NB colonies sharing the same profiles had
535 different susceptibilities in M0. During the peak of the heatwave in Oct-2014 (M0) Pcom_NB
536 associated to DIVs C15cc and D6, and more often to the ITS2 profile C15-C5ci-C15cc-C15cl-
537 C15n-C15cj-C15l, which could represent a thermotolerant symbiont-type found in 7 out of 10
538 resistant colonies, and in only one susceptible Pcom_B. Accordingly, this profile was less
539 prevailing in M6 (May 2015), coinciding with a period of minor thermal disturbances and lower
540 symbiont abundances (Brown et al., 1999; Cunning et al., 2015). C15-genotypes with higher
541 temperature tolerance were already described associating to *Porites* spp. from the Great Barrier
542 Reef (Fisher et al., 2012). Dissimilarities in ITS2-sequences between Pcom_B and Pcom_NB
543 tended to vanish after M1, reflecting algal rearrangements linked to recovery from this time
544 point. This concurs with coral photo-physiology data supporting intense symbiont repopulation
545 (elevated cell mitosis and photopigment synthesis) from Nov (Wall et al., 2019; Matsuda et al.,
546 2020; Ritson-Williams and Gates 2020).
547 Bacterial communities in Pcom were less diverse than in the other hosts, accounting for
548 many low abundance taxa, and ~ 90 % predominance of a single *Endozoicomonas* microbe. The
549 bacterial community structures were relatively constant, across bleaching phenotypes and time.
550 Salerno et al. (2011) also found stable microbiomes in *P. compressa* under mild thermal
551 treatments; whereas Vega Thurber et al. (2009) observed switches from healthy to pathogenic
552 microbiota after intense high temperature exposures. Both of these thermal stresses were

553 administered in an experimental setting. In our field data the prevalent ASV
554 (694df3c7f8b6b66c922ed51a965d75d0a) matched with a symbiont (Oceanospirillaceae-OTU
555 C7-A01: FJ930289.1; Supplementary Material S2) broadly documented in *Porites* spp.
556 (including *P. compressa* from Maui) and other hermatypic corals from Australia, Hawai'i, and
557 Bermuda (Speck and Donachie 2012), suggesting a conserved large-scale partnership with
558 corals (Neave et al., 2016). Coral-microbiomes dominated by one or few *Endozoicomonas*
559 phylotypes were described to have microbial inflexibility in stress responses (Pogoreutz et al.,
560 2018). In our susceptible Pcom_B corals dominated by one *Endozoicomonas* strain though, the
561 microbial balance composed by two *Endozoicomonas* (the predominant ASV above and another
562 congeneric strain), *Candidatus Amoebophilus, Acinetobacter calcoaceticus, Pseudosmonas*
563 *stutzeri, Synechococcus* and *Roseitalea* phylotypes; over five antagonistic *Endozoicomonas*
564 strains*, Micrococcus, Staphylococcus* and Neisseriaceae taxa, pinpointed a longitudinal
565 discontinuity of increased log-ratios in Pcom_B at M1. Microbial communities of bleaching
566 resistant Pcom_NB phenotypes, in contrast, remained stable and dominated by
567 *Endozoicomonas*. Different from Pogoreutz and co-workers (2018) findings, the relative
568 microbial inflexibility of Pcom and *Endozoicomonas* predominance, could afford benefits in
569 terms of resistance or faster recovery during thermal stress responses.
570 Pcom was characterized by small cross networks with mild fluctuations between
571 heatwaves, reflecting a much simpler microbial community. Increased edge complexity at M1
572 in Pcom_B again suggests a rapid recovery response, with reliance on few bacterial ASVs; as
573 compared to Mcap_B and Pacu_B, reflecting larger bacterial consortia participating in the
574 recovery. Reduced trophic plasticity, and intense loss of Symbiodiniaceae and photosynthetic
575 pigments might obligate Pcom_B to regain symbionts faster, at high biomass investment with
576 respect to the other species (Wall et al., 2019; Matsuda et al., 2020). Furthermore, intense algal
577 repopulation in Pcom_B from October–November 2014 was correlated with low symbiont $\partial^{15}N$
578 (Wall et al., 2019), and assimilation of ^{15}N depleted sources, possibly derived from diazotroph
579 bacteria via N_2 fixation (Lesser et al., 2007; Cardini et al., 2015; Bednarz et al., 2017). Indeed,

differentially abundant taxa ranked to recovering Pcom_B included various diazotroph taxa (see below).

4.4. Differentially abundant bacterial taxa defining temporal shifts in bleaching recovery

Coral microbiomes in the present study revealed minor community disruption in response to heatwaves. Similar outcomes were reported previously, together with increases in potentially beneficial (Santos et al., 2014; Epstein et al., 2019). One bacterial group widely associated to corals and documented to display diversified tolerances and/or functional traits to stress conditions is *Endozoicomonas* (Bourne et al., 2005; Vega Thurber et al., 2009; Littman et al., 2011; Neave et al., 2016; McDevitt-Irwin et al., 2017; Pogoreutz et al., 2018; Ziegler et al., 2016, 2017, 2019; Epstein et al., 2019). In our corals, saving an initial decline in Mcap_B at M0, this genus displayed preponderance throughout bleaching stress, in agreement with other studies (Ziegler et al., 2016; Pogoreutz et al., 2018; Epstein et al., 2019). *Endozoicomonas* symbionts are proposed to play three kinds of functions: 1) nutrient acquisition/provision – carbon, nitrogen, sulphur, methane recycling, amino acid production, dimethylsulfoniopropionate (DMSP) metabolism; 2) microbiome modulation –quorum-sensing; and 3) promotion of host health –antimicrobial activity, pathogens exclusion (Neave et al., 2016, 2017). DMSP produced by Symbiodiniaceae and sulfur-derivatives from certain prokaryotes (*Endozoicomonas*, *Acinetobacter*, *Pseudomonas*, *Vibrio*) provide a selective environment structuring bacterial populations (Raina et al., 2010). Hence, upon the downturn of DMSP production throughout bleaching/stress episodes, high abundances of *Endozoicomonas* might modulate microbiomes steadiness (Ziegler et al., 2016; Pogoreutz et al., 2018; Epstein et al., 2019). Further, diazotroph bacteria contribute to homeostasis during bleaching and sub-bleaching recovery after thermal stress (Santos et al., 2014; Epstein et al., 2019), by suppling limiting nitrogen to Symbiodiniaceae (Lesser et al., 2007; Olson et al., 2009; Cardini et al., 2015; Bednarz et al., 2017). Indeed, many differentially abundant taxa positively ranked to our recovering corals included diazotrophs and/or DMSP-metabolizing bacteria: e.g.,

608 *Endozoicomonas, Acinetobacter calcoaceticus*, *Pseudomonas stutzeri, Cyanobium* (Lalucat et
609 al., 2006; Lesser et al., 2007; Olson et al., 2009; Raina et al., 2010). High occurrence of
610 *Acinetobacter* spp. and *Endozoicomonas* spp. is frequently documented in healthy and bleached
611 Scleractinia, implying synergistic roles in fitness (Cai et al., 2018). Another recently described
612 symbiont in coral holobionts is *Candidatus Amoebophilus*, an intracellular associate of
613 unicellular eukaryotes, like Symbiodiniaceae or amoebae, with undefined role (Huggett and
614 Apprill 2018; Epstein et al., 2019). Differential phylotypes in this genus were correlated to algal
615 repopulation, particularly in Pcom_B. Bleaching entails loss of major nourishment inputs and
616 photoprotection, and corals therefore implement compensatory strategies (Fitt et al., 2001). For
617 instance, bleached corals have been observed to reinforce feeding on planktonic diazotrophs and
618 preferentially on nitrogen-rich *Synechococcus* cyanobacteria (Meunier et al., 2019).
619 Accordingly, bleached colonies and incipient recovery stages in this study were associated to
620 *Synechococcus*; but interestingly also to differential phylotypes with potential UV-absorbing
621 properties, like *Bacillus*, *Staphylococcus* (Ravindran et al., 2013), *Micrococcus* (Arai et al.,
622 1992), and the already mentioned Cyanobacteria –*Cyanobium, Synechococcus* (Sinha et al.,
623 2001). Notably, *Bacillus* and *Staphylococcus* strains within the coral mucus have demonstrated
624 to increase their UV-absorbance range in response to elevated temperatures, likely protecting
625 bleached colonies from excessive irradiation prior to recovery (Ravindran et al., 2013).
626 *Lawsonella* was another genus frequently associated with bleached corals here. Despite little
627 information exists on marine representatives, it could involve opportunistic/transient microbes,
628 as those described in certain human abscesses (Bell et al., 2016). Differentially abundant taxa
629 were broadly shared between Mcap and Pacu, and partially matching with Pcom –this last
630 chiefly influenced by *Endozoicomonas* spp. This outcome is appealing, and suggests that locally
631 the same players may modulate stress responses in different coral species. Thus, understanding
632 the dynamics of differentially abundant microbial consortia in correlation with bleaching and
633 recovery, could provide regional indicators to forecast the fate of sympatric corals to upcoming
634 (Glasl et al., 2017). Furthermore, certain strains could be proposed as "probiotics" to improve
635 coral resistance (Peixoto et al., 2017).

5. Conclusions

Prokaryotic and algal microbiomes differed among the three coral species. Despite the recovery of the bleached individuals, there was no apparent pattern of temporal acclimatization. Symbiodiniaceae shifts were found by bleaching phenotype in Mcap and Pcom, probably contributing to resistance. Compared to previous work, ITS2-type profiling (Hume et al., 2019) allowed us to disentangle higher intraspecific resolution within Symbiodiniaceae diversity. Whist compositional analyses (Morton et al., 2019) on the other, permitted the identification of fine-scale differences in the abundance of certain ASVs/DIVs driving changes by bleaching susceptibility and time within each host, despite overall stability of the communities. Fungal associates remain unexplored, until better methods can address host co-amplification and improve taxonomic identifications (Amend et al., 2012).

The three major coral reef founders in Kane'ohe Bay revealed different responses after 2014–2015 heatwaves. Pacu had thorough bleaching susceptibility and recovered photosynthetic symbionts probably relying on heterotrophy (Lyndby et al., 2020; Dobson et al., 2021), and microbiome rearrangements in the early recovery phases (Santos et al., 2014; Ziegler et al., 2017). Mcap and Pcom displayed two bleaching phenotypes, and the susceptible colonies Mcap_B revealed greater bleaching resistance and slower recovery at low biomass investment. Instead, Pcom_B underwent stronger bleaching (higher pigment loss), faster symbiont repopulation at higher metabolic expenses, but attained better energetic standing (Wall et al., 2019; Ritson-Williams and Gates 2020).

It is difficult to forecast which of the three strategies will become successful in future scenarios. Yet, after the recent 2019 heatwave in Hawai'i *P. compressa* demonstrated better performance than *M. capitata*, suggesting certain acclimatization (Innis et al., 2018; Matsuda et al., 2020). Similarly, poritid corals from Panamá predicted to be disadvantaged to upcoming

climate and anthropogenic disturbances with respect to other co-dominant scleractinians (Aronson et al., 2014), have demonstrated unexpected resilience (O'Dea et al., 2020). Cumulative research demonstrates that coral responses to thermal stress are reliant on host species, geography, and severity/frequency of the events, impeding the elaboration of generalizations. Notwithstanding this limitation, further understanding on microbial balances, may allow to identify finer scale taxa dynamics as local indicators of coral reef fitness (Glasl et al., 2017; Peixoto et al., 2017), serving as diagnostic tools for ecosystem stress.

Appendix A. Supplementary data

S1. Núñez-Pons_et_alii_S1_SupplementaryMethods: **Coral bleaching monitoring. Experimental co-variates**: **Table S1.** Experimental co-variates information. **Bioinformatics analysis. Sequencing outputs: Table S2A.** Sequencing outputs of 16S rRNA gene V_4 reads. **Table S2B**. Sequencing outputs of ITS1reads. **Table S2C**. Sequencing outputs of ITS2 reads. **Rarefaction and sequencing depth: Table S3A**. Rarefaction information for 16S rRNA data, **Table S3B.** Rarefaction information for ITS1 data, **Table S3C.** Rarefaction information for ITS1 data.

S2. Núñez-Pons_et_alii_S2_SupplementaryResults: **Alpha diversity for 16s rRNA gene data. Fig. S1.** Alpha diversity. **Beta diversity for 16s rRNA gene data. Fig. S2.1.** RPCA compositional biplot based on Aitchison distances for Mcap. **Fig. S2.2.** RPCA compositional biplots based on Aitchison distances for Pcom. **Fig. S2.3.** RPCA compositional biplots based on Aitchison distances for Pacu. **Taxa bar plots at ASV level. Fig. S.3.1.** Prokaryotic composition at the ASV level for Mcap. **Fig. S.3.2.** Prokaryotic composition at the ASV level for Pcom. **Fig. S.3.2.** Prokaryotic composition at the ASV level for Pacu. **Longitudinal approaches. Longitudinal analyses for the 16S rRNA gene data**. **Fig S4.1.** Box plot of pairwise distances on Jaccard index of 16S data. **Fig S4.2.** Box plot of pairwise distances on Bray Curtis beta index of 16S data. **Fig S4.3.** Volatility plot on Bray Curtis distances of 16S data from one timepoint to

690 the consecutive. **Fig S4.4.** Volatility based on Bray Curtis distances of 16S data on coral
691 colonies from any time point respect to M0. **Fig S4.5.** Volatility plot of shared phylotypes of
692 16S data from any time point respect to M0. **Fig S4.6.** Volatility plot on log-ratio rakings of
693 microbial bacterial balances formed by differential taxa from one timepoint to the consecutive.
694 **Fig S4.7.** Volatility on log-ratio rakings of microbial bacterial balances formed by differential
695 taxa from any time point respect to Month 0. **Longitudinal analyses for the ITS2 data**. **Fig.**
696 **S4.8.** Volatility plots of first distances with DEICODE of ITS2 sequences from any time point
697 to Month 0. **Fig. S4.9.** Volatility plots of first distances with Bray Curtis from any time point to
698 Month 0 for ITS2 sequences. **Fig. 4.10.** Pairwise differences on LogRatios of balances formed
699 by differential ITS2 sequences in Pcom. **Fig. S4.11.** Pairwise differences on LogRatios of
700 balances formed by differentially abundant ITS2 sequences between Month 0 and 6. **Fig. 4.12**
701 Volatility plot of log-ratios ranks of balances formed by differential ITS2 sequences from corals
702 across time points M0–M6. **Longitudinal trajectories of differential bacterial taxa. Fig S5**.
703 Longitudinal trajectory plots of CLR of differential *Endozoicomonas* microbes in Pcom. **Fungal**
704 **community inspection. Fig. S6.** Taxa bar plots for the ITS1 data annotated at the Kingdom
705 level. **Cross co-occurrence networks analysis. Fig. 6.** Cross co-occurrence networks of ASV
706 bacteria phylotypes *vs* ITS2 type profiles with annotated taxonomy. **Genetic BLAST**
707 **alignment of prevalent *Endozoicomonas*.**
708
709 S3. Núñez-Pons_et_alii_S3_SupplementaryStatsTables: **Alpha diversity statistics for 16s**
710 **rRNA gene data. Table S4A.** Shannon by coral species. **Table S4B.** Shannon by coral species
711 and bleaching susceptibility. **Table S4C.** Shannon by coral species, bleaching susceptibility and
712 time point. **Table S4D.** Observed phylotypes by coral species. **Table S4E.** Observed phylotypes
713 by coral species and bleaching susceptibility. **Table S4F.** Observed phylotypes by coral species,
714 bleaching susceptibility and time point. **Table S4G.** Pielou's Evenness by coral species. **Table**
715 **S4H.** Pielou's Evenness by coral species and bleaching susceptibility. **Table S4I.** Pielou's
716 Evenness by coral species, bleaching susceptibility and time point. **Beta diversity statistics for**
717 **16s rRNA gene data. Table. 5A:** DEICODE beta diversity across coral species and TimePoint.

718 **Table. 5B:** Bray Curtis beta diversity across coral species and TimePoint. **Table. 5C:** Jaccard
719 beta diversity across coral species and TimePoint. **Table 6A:** DEICODE by bleaching
720 susceptibility across time points. **Table 6B:** Bray Curtis by bleaching susceptibility across time
721 points. **Table 6C:** Jaccard by bleaching susceptibility across time points. **Table 7A:** Beta
722 diversity comparisons based on DEICODE between bleaching susceptible coral phenotypes.
723 **Table 7B:** Beta diversity comparisons based on Bray Curtis between bleaching susceptible
724 coral phenotypes. **Table 7C:** Beta diversity comparisons based on Jaccard between bleaching
725 susceptible coral phenotypes. **Beta diversity statistics for ITS2 data. Table 9A:** DEICODE
726 beta diversity for ITS2 profiles across species and by Bleaching susceptibility. **Table 9B:** Bray
727 Curtis beta diversity for ITS2 profiles across species and by Bleaching susceptibility. **Table 9C:**
728 Jaccard beta diversity for ITS2 profiles across species and by Bleaching susceptibility. **Table**
729 **10A:** DEICODE beta diversity comparisons of differential ITS2 DIVs sequences across coral
730 species and by Bleaching susceptibility. **Table 10B:** Bray Curtis beta diversity comparisons of
731 differential ITS2 DIVs sequences across coral species and by Bleaching susceptibility. **Table**
732 **10C:** Jaccard beta diversity comparisons of differential ITS2 DIVs sequences across coral
733 species and by Bleaching susceptibility. **Table 11A:** Beta diversity comparisons based on
734 DEICODE distances on differential ITS2 DIVs sequences by bleaching susceptibility across
735 time points. **Table 11B:** Beta diversity comparisons based on Bray Curtis distances on
736 differential ITS2 DIVs sequences by bleaching susceptibility across time points. **Table 11C:**
737 Beta diversity comparisons based on Jaccard distances on differential ITS2 DIVs sequences by
738 bleaching susceptibility across time points. **Table 12A.** Beta diversity comparisons based on
739 DEICODE distances for differential ITS2 DIVs sequences by bleaching susceptibility and time
740 point. **Table 12B.** Beta diversity comparisons based on Bray Curtis distances for differential
741 ITS2 DIVs sequences by bleaching susceptibility and time point. **Table 12C.** Beta diversity
742 comparisons based on Jaccard distances for differential ITS2 DIVs sequences by bleaching
743 susceptibility and time point.
744

S4. Núñez-Pons_et_alii_S4_SupplementaryDiffAbundTables16S: **Table S8A.** Differential bacterial taxa for Mcap_B across all time points. **Table S8b.** Differential bacterial taxa for Mcap_NB across all time points. **Table S8C.** Differential bacterial taxa for Pcom_B across all time points. **Table S8D.** Differential bacterial taxa for Pcom_NB across all time points. **Table S8E.** Differential bacterial taxa for Pacu_B across all time points. **Table S8F.** Differential bacterial taxa Mcap B and NB by time points M0–M12. **Table S8G.** Differential bacterial taxa Pcom B and NB by time points M0–M12.

S5. Núñez-Pons_et_alii_S5_ SupplementaryDiffAbundTablesITS2: **Table S13A.** Differential ITS2 sequence DIVs for Mcap across all time points. **Table S13B.** Differential ITS2 sequence DIVs for Pcom across all time points. **Table S13C.** Differential ITS2 sequence DIVs for Pacu across all time points. **Table S13D.** Differential ITS2 sequence DIVs for Mcap B and NB in time points M0–M6. **Table S13E.** Differential ITS2 sequence DIVs for Pcom B and NB in time points M0–M6.

CRediT authorship contribution statement

Laura Núñez-Pons: Conceptualization; Data curation; Formal analysis; Funding acquisition; Investigation; Methodology; Project administration; Resources; Software; Supervision; Validation; Visualization; Writing - original draft. **Ross Cunning:** Methodology; Validation; Visualization; Writing - review & editing. **Craig Nelson:** Conceptualization; Data curation; Methodology; Resources; Supervision. **Anthony Amend:** Conceptualization; Methodology; Resources; Validation. **Emilia M. Sogin:** Methodology; Validation. **Ruth Gates:** Conceptualization; Funding acquisition; Project administration; Resources. **Raphael Ritson-Williams:** Conceptualization; Investigation; Methodology; Project administration; Resources; Supervision; Writing - review & editing.

Declaration of competing interest

The authors have no conflicts of interest to declare.

Acknowledgements

Thanks are due to C. Wall, L. Benz, K. Barrot, for fieldwork assistance; L. Orlando and D. Pons Romaní for logistics and support, V. Mazzella and L. Pfingsten for formatting handout. We are thankful to A. Eggers and M. Mizobe from the sequencing facility at the Core Lab in HIMB. Experiment.com all-or-nothing crowdfunding platform (https://experiment.com) allowed to obtain part of the funding for sequencing related costs, and we acknowledge all the trustful project backers and supporters (project: https://experiment.com/projects/stayin-alive-how-do-microbes-help-corals-recover-from-bleaching?s=search).

Author information

Authors and affiliations

[1] *Department of Integrative Marine Ecology (EMI), Stazione Zoologica Anton Dohrn, Villa Comunale, 80121 Napoli, Italy.*

[2] *NBFC, National Biodiversity Future Center, Palermo 90133, Italy*

Laura Núñez-Pons: laura.nunezpons@szn.it

[3] *Daniel P. Haerther Center for Conservation and Research, John G. Shedd Aquarium, 1200 South Lake Shore Drive, Chicago, IL 60605, USA.*

Ross Cunning: rcunning@sheddaquarium.org

[4] *Sea Grant College Program, University of Hawai'i at Mānoa, Honolulu, HI, USA.*

Craig Nelson: craig.nelson@hawaii.edu

[5] *Pacific Biosciences Research Center, University of Hawai'i at Mānoa, Honolulu, HI 96822, USA.*

Anthony Amend: amend@hawaii.edu

[6] *Molecular and Cell Biology, University of California Merced, Merced, CA, USA.*

Emilia M. Sogin: esogin@ucmerced.edu

[7] *Hawai'i Institute of Marine Biology, University of Hawai'i at Mānoa, Honolulu, HI, USA.*

Ruth Gates: rgates@hawaii.edu

[8] *College of Arts and Sciences, The Heart of Santa Clara University, Vari Hall 500 El Camino Real Santa Clara, CA 95053, USA.*

Raphael Ritson-Williams: rritson-williams@calacademy.org

Corresponding author

Correspondence to Laura Núñez-Pons: laura.nunezpons@szn.it.

Data availability

Sequencing data and associated metadata are available at National Center for Biotechnology Information (NCBI, Genbank) under BioProject PRJNA791513 for 16S rRNA gene, BioProject PRJNA794040 for ITS1, and BioProject PRJNA794042 for ITS2 data. Other data will be made available by contacting the corresponding author.

References

Ainsworth T, Gates R. Corals' microbial sentinels. Science. 2016;352:1518–19. doi: d10.1126/science.aad9957.

Ainsworth T, Krause L, Bridge T, Raina JB, Zakrzewski M, Gates RD et al. The coral core microbiome identifies rare bacterial taxa as ubiquitous endosymbionts. ISME J. 2015;9:2261–74. doi: 10.1038/ismej.2015.39.

Ainsworth TD, Renzi JJ, Silliman BR. Positive interactions in the coral macro and microbiome. Trends Microbiol. 2020;28(8):602–4. doi: 10.1016/j.tim.2020.02.009.

Aitchison J. The statistical analysis of compositional data. J. R. Stat. Soc. Ser. B Methodol. 1982;44(2):139–60. doi: 10.1111/j.2517-6161.1982.tb01195.x.

Amend A, Barshis D, Oliver T. Coral-associated marine fungi form novel lineages and heterogeneous assemblages. ISME J. 2012;6:1291–301. doi: 10.1038/ismej.2011.193

826 Apprill A, McNally S, Parsons R, Weber L. Minor revision to V4 region SSU rRNA 806R gene
827 primer greatly increases detection of SAR11 bacterioplankton. Aquat. Microb. Ecol.
828 2015;75(2):129–37. doi: 10.3354/ame01753.
829 Arai T, Nishijima M, Adachi K, Sano H. Isolation and structure of UV absorbing substance
830 from the marine bacterium Micrococcus sp. AK-334. MBI Report. Marine Biotechnology
831 Institute, Tokyo, Japan; 1992; p 88–94.
832 Aronson RB, Hilbun NL, Bianchi TS, Filley TR, McKee BA. Land use, water quality, and the
833 history of coral assemblages at Bocas del Toro, Panamá. Mar. Ecol. Prog. Ser.
834 2014;504:159–70. doi: 10.3354/meps10765.
835 Bahr KD, Jokiel PL, Toonen RJ. The unnatural history of Kāne'ohe Bay: coral reef resilience in
836 the face of centuries of anthropogenic impacts. PeerJ. 2015;3:e950. doi: 10.7717/peerj.950.
837 Baird AH, Bhagooli R, Ralph PJ, Takahashi S. Coral bleaching: the role of the host. Trends
838 Ecol. Evol. 2009;24:16–20. doi: 10.1016/j.tree.2008.09.005.
839 Baker AC. Flexibility and specificity in coral-algal symbiosis: diversity, ecology, and
840 biogeography of *Symbiodinium*. Annu. Rev. Ecol. Evol. Syst. 2003;34:661–89. doi:
841 10.1146/annurev.ecolsys.34.011802.132417
842 Baker AC. Reef corals bleach to survive change. Nature. 2001;411:765–6. doi:
843 10.1038/35081151.
844 Bednarz VN, Grover R, Maguer J-F, Fine M, Ferrier-Pagès C. The assimilation of diazotroph-
845 derived nitrogen by scleractinian corals depends on their metabolic status. MBio.
846 2017;8:e02058–e02016. doi:10.1128/mBio.02058-16.
847 Bell ME, Bernard KA, Harrington SM, Patel NB, Tucker T-A, Metcalfe M G, et al. *Lawsonella*
848 *clevelandensis* gen. nov., sp. nov., a new member of the suborder Corynebacterineae
849 isolated from human abscesses. Int. J. Syst. Evol. Microbiol. 2016;66:2929–35. doi:
850 10.1099/ijsem.0.001122.
851 Berkelmans R, van Oppen MJH. The role of zooxanthellae in the thermal tolerance of corals: a
852 'nugget of hope' for coral reefs in an era of climate change. Proc. R. Soc. B.
853 2006;273:2305–12. doi: 10.1098/rspb.2006.3567.

Beurmann S, Ushijima B, Videau P, Svoboda CM, Chatterjee A, Aeby GS et al. Dynamics of acute *Montipora* white syndrome: bacterial communities of healthy and diseased *M. capitata* colonies during and after a disease outbreak. Microbiology (Reading, Engl.). 2018;164(10):1240-53. doi: 10.1099/mic.0.000699.

Boilard A, Dubé CE, Gruet C, Mercière A, Hernandez-Agreda A, Derome N. Defining coral bleaching as a microbial dysbiosis within the coral holobiont. Microorganisms. 2020;8(11):1682. doi:10.3390/microorganisms8111682.

Bokulich NA, Dillon M, Bolyen E, Kaehler BD, Huttley GA, Caporaso JG. q2-sample-classifier: machine-learning tools for microbiome classification and regression. J. Open Source Softw. 2018;3:934. doi: 10.21105/joss.00934.

Bokulich NA, Dillon MR, Zhang Y, Rideout R, Bolyen E, Li H, et al. q2-longitudinal: longitudinal and paired-sample analyses of microbiome data. mSystems. 2018;3:1–9. doi: 10.1128/mSystems.00219-18.

Bokulich NA, Kaehler BD, Rideout JR, Dillon M, Bolyen E, Knight R, et al. Optimizing taxonomic classification of marker-gene amplicon sequences with QIIME 2's q2-feature-classifier plugin. Microbiome. 2018;6:1–17. doi: 10.1186/s40168-018-0470-z.

Bolyen E, Rideout JR, Dillon MR, Bokulich NA, Chase J, Cope EK, et al. Reproducible, interactive, scalable and extensible microbiome data science using QIIME 2. Nat. Biotechnol. 2019;37:852–7. doi: 10.1038/s41587-019-0209-9.

Bourne DG, Morrow KM, Webster NS. Insights into the coral microbiome: underpinning the health and resilience of reef ecosystems. Annu. Rev. Microbiol. 2016;70:317–40. doi: 10.1146/annurev-micro-102215-095440.

Bourne DG, Munn CB. Diversity of bacteria associated with the coral *Pocillopora damicornis* from the Great Barrier Reef. Environ. Microbiol. 2005;7(8):1162–74. doi: 10.1111/j.1462-2920.2005.00793.x.

Brener-Raffalli K, Clerissi C, Vidal-Dupiol J, Adjeroud M, Bonhomme F, Pratlong M et al. Thermal regime and host clade, rather than geography, drive Symbiodinium and bacterial

881 assemblages in the scleractinian coral *Pocillopora damicornis* sensu lato. Microbiome.
882 2018;6:39. doi: 10.1186/s40168-018-0423-6.
883 Brown BE, Dunne RP, Ambarsari I, LeTissier MDA, Satapoomin U. Seasonal fluctuations in
884 environmental factors andvariations in symbiotic algae and chlorophyllpigments in four
885 Indo-Pacific coral species. Mar. Ecol. Prog. Ser. 1999;191:53–69. doi:
886 10.3354/meps191053.
887 Cai L, Tian RM, Zhou G, Tong H, Wong YH, Zhang W et al. Exploring coral microbiome
888 assemblages in the South China Sea. Sci. Rep. 2018;8:2428. doi:10.1038/s41598-018-
889 20515-w.
890 Callahan BJ, Mcmurdie PJ, Rosen MJ, Han AW, Johnson AJ, Holmes SP. DADA2: High
891 resolution sample inference from amplicon data. Nat. Methods. 2016;13:581–3. doi:
892 10.1038/nmeth.3869.
893 Caporaso JG, Lauber CL, Walters WA, Berg-Lyons D, Huntley J, Fierer N, et al. Ultra-high-
894 throughput microbial community analysis on the Illumina HiSeq and MiSeq platforms.
895 ISME J. 2012;6:1621–24. doi: 10.1038/ismej.2012.8.
896 Cardini U, Bednarz VN, Naumann MS, van Hoytema N, Rix Z, Foster RA et al. Functional
897 significance of dinitrogen fixation in sustaining coral productivity under oligotrophic
898 conditions. Proc. Biol. Sci. 2015;282:2257. doi: 10.1098/rspb.2015.2257.
899 Conti-Jerpe IE, Thompson PD, Wong CWM, Oliveira NL, Duprey NN, Moynihan MA et al.
900 Trophic strategy and bleaching resistance in reef-building corals. Sci. Adv.
901 2020;10:6(15):eaaz5443. doi: 10.1126/sciadv.aaz5443.
902 Cunning R, Ritson-Williams R, Gates RD. Patterns of bleaching and recovery of *Montipora*
903 *capitata* in Ka¯ne‘ohe Bay, Hawai’i, USA. Mar. Ecol. Prog. Ser. 2016;551:131–9. doi:
904 10.3354/meps11733.
905 Cunning R, Silverstein RN, Baker AC. Investigating the causes and consequences of symbiont
906 shuffling in a multi-partner reef coral symbiosis under environmental change. Proc. R. Soc.
907 B. 2015;282:20141725. doi: 10.1098/rspb.2014.1725.

908 D'Angelo C, Hume B, Burt J, Smith EG, Achterberg EP, Wiedenmann J. Local adaptation
909 constrains the distribution potential of heat-tolerant *Symbiodinium* from the Persian/Arabian
910 Gulf. ISME J. 2015;9:2551–60. doi: 10.1038/ismej.2015.80.
911 Dobson KL, Ferrier-Pagès C, Saup CM, Grottoli AG. The effects of temperature, light, and
912 feeding on the physiology of *Pocillopora damicornis*, *Stylophora pistillata*, and *Turbinaria*
913 *reniformis* corals. Water. 2021;13(15):2048. doi: 10.3390/w13152048.
914 Douglas AE. Coral bleaching—how and why? Mar. Pollut. Bull. 2003;46:385–92. doi:
915 10.1016/S0025-326X(03)00037-7.
916 Edmunds PJ. Evidence that reef-wide patterns of coral bleaching may be the result of the
917 distribution of bleaching- susceptible clones. Mar. Biol. 1994;121:137–42. doi:
918 10.1007/BF00349482
919 Epstein HE, Torda G, van Oppen MJ. Relative stability of the *Pocillopora acuta* microbiome
920 throughout a thermal stress event. Coral Reefs. 2019;38:373–86. doi: 10.1007/s00338-019-
921 01783-y.
922 Falkowski PG, Dubinsky Z, Muscatine L, Porter JW. Light and the bioenergetics of a symbiotic
923 coral. Bioscience. 1984;34:705–9. doi: 10.2307/1309663.
924 Fedarko MW, Martino C, Morton JT, González A, Rahman G, Marotz CA, et al. Visualizing
925 'omic feature rankings and log-ratios using Qurro. NAR genom. bioinform. 2020;2:1–7.
926 doi: 10.1093/nargab/lqaa023.
927 Fisher PL, Malme MK, Dove S. The effect of temperature stress on coral–Symbiodinium
928 associations containing distinct symbiont types. Coral Reefs. 2012;31:473–485. doi:
929 10.1007/s00338-011-0853-0.
930 Fitt WK, Brown BE, Warner ME, Dunne RP. Coral bleaching: interpretation of thermal
931 tolerance limits and thermal thresholds in tropical corals. Coral Reefs. 2001;20:51–65. doi:
932 10.1007/s003380100146.
933 Franklin EC, Stat M, Pochon X, Putnam HM, Gates RD. GeoSymbio: a hybrid, cloud-based
934 web application of global geospatial bioinformatics and ecoinformatics for *Symbiodinium*-

935 host symbioses. Mol. Ecol. Resour. 2012;12:369–373. doi: 10.1111/j.1755-
936 0998.2011.03081.x.
937 Gardes M, Bruns TD. ITS primers with enhanced specificity for basidiomycetes--application to
938 the identification of mycorrhizae and rusts. Mol. Ecol. 1993;2(2):113–8. doi:
939 10.1111/j.1365-294x.1993.tb00005.x.
940 Gardner SG, Camp EF, Smith DJ, Kahlke T, Osman EO, Gendron G. et al. Coral microbiome
941 diversity reflects mass coral bleaching susceptibility during the 2016 El Niño heat wave.
942 Ecol. Evol. 2019;9(3):938–56. doi: 10.1002/ECE3.4662.
943 Glasl B, Webster NS, Bourne DG. Microbial indicators as a diagnostic tool for assessing water
944 quality and climate stress in coral reef ecosystems. Mar. Biol. 2017;164:1–18. doi:
945 10.1007/s00227-017-3097-x.
946 Glynn PW, Mate-T JL, Baker AC, Calderón MO. Coral bleaching and mortality in Panamá and
947 Ecuador during the 1997-1998 El Niño southern oscillation event: spatial/temporal patterns
948 and comparisons with the 1982-1983 event. Bull. Mar. Sci. 2001;69 (1):79–109.
949 Grottoli A, Rodrigues L, Palardy J. Heterotrophic plasticity and resilience in bleached corals.
950 Nature. 2006;440:1186–9. doi: 10.1038/nature04565
951 Grottoli AG, Warner ME, Levas SJ, Aschaffenburg MD. The cumulative impact of annual coral
952 bleaching can turn some coral species winners into losers. Glob. Change Biol.
953 2014;20:3823–33. doi: 10.1111/gcb.12658.
954 Hernandez-Agreda A, Gates RD, Ainsworth TD. Defining the core microbiome in corals'
955 microbial soup. Trends Microbiol. 2017;25(2):125-40. doi: 10.1016/j.tim.2016.11.003.
956 Hernandez-Agreda A, Leggat W, Bongaerts P, Herrera C, Ainsworth TD. Rethinking the coral
957 microbiome: simplicity exists within a diverse microbial biosphere. mBio.
958 2018;9(5):e00812-18. doi: 10.1128/mBio.00812-18.
959 Howells EJ, Bauman AG, Vaughan GO, Hume BCC, Voolstra CR, Burt JA. Corals in the
960 hottest reefs in the world exhibit symbiont fidelity not flexibility. Mol. Ecol. 2020;29: 899–
961 911. doi: 10.1111/mec.15372.

962 Huggett MJ, Apprill A. Coral microbiome database: integration of sequences reveals high
963 diversity and relatedness of coral-associated microbes. Environ. Microbiol. Rep.
964 2019;11:372–85. doi: 10.1111/1758-2229.12686.
965 Hughes AD, Grottoli AG. Heterotrophic compensation: a possible mechanism for resilience of
966 coral reefs to global warming or a sign of prolonged stress? PLoS One. 2013;8(11):e81172.
967 doi: 10.1371/journal.pone.0081172.
968 Hume B, D'Angelo C, Smith E, Stevens JR, Burt J, Wiedenmann J. *Symbiodinium*
969 *thermophilum* sp. nov., a thermotolerant symbiotic alga prevalent in corals of the world's
970 hottest sea, the Persian/Arabian Gulf. Sci. Rep. 2015;5:8562. doi: 10.1038/srep08562.
971 Hume BC, Mejia-Restrepo A, Voolstra CR, Berumen ML. Fine-scale delineation of
972 Symbiodiniaceae genotypes on a previously bleached central Red Sea reef system
973 demonstrates a prevalence of coral host-specific associations. Coral Reefs. 2020;39:583–
974 601. doi: 10.1007/s00338-020-01917-7.
975 Hume BCC, Smith EG, Ziegler M, Warrington M, Burt JA, LaJeunesse TC et al. SymPortal: A
976 novel analytical framework and platform for coral algal symbiont next-generation
977 sequencing ITS2 profiling. Mol. Ecol. Resour. 2019;9:1063–80. doi: 10.1111/1755-
978 0998.13004.
979 Innis T, Cunning R, Ritson-Williams R, Wall CB, Gates RD. Coral color and depth drive
980 symbiosis ecology of *Montipora capitata* in Kāne`ohe Bay, O`ahu, Hawai`i. Coral Reefs.
981 2018;37(2):423–30. doi:10.1007/s00338-018-1667-0.
982 Jokiel PL. Temperature stress and coral bleaching. In: Rosenberg E, Loya Y, eds. Coral health
983 and disease. Heidelberg: Springer-Verlag 2004;401–25.
984 Kozich JJ, Westcott SL, Baxter NT, Highlander SK, Schloss PD. Development of a dual-index
985 sequencing strategy and curation pipeline for analyzing amplicon sequence data on the
986 MiSeq Illumina sequencing platform. Appl. Environ. Microbiol. 2013;79:5112–20. doi:
987 10.1128/AEM.01043-13.

LaJeunesse TC, Parkinson JE, Gabrielson PW, Jeong HJ, Reimer JD, Voolstra CR et al. Systematic Revision of Symbiodiniaceae Highlights the Antiquity and Diversity of Coral Endosymbionts. Curr. Biol. 2018;28(16):2570–80.e6. doi: 10.1016/j.cub.2018.07.008.

LaJeunesse TC, Thornhill DJ, Cox EF, Stanton FG, Fitt WK, Schmidt GW. High diversity and host specificity observed among symbiotic dinoflagellates in reef coral communities from Hawaii. Coral Reefs. 2004;23:596–603. doi: 10.1007/S00338-004-0428-4.

LaJeunesse TC, Thornhill DJ, Cox EF, Stanton FG, Fitt WK, Schmidt GW. High diversity and host specificity observed among symbiotic dinoflagellates in reef coral communities from Hawaii. Coral Reefs. 2004;23:596–603. doi: 10.1007/S00338-004-0428-4.

Lalucat J, Bennasar A, Bosch R, García-Valdés E, Palleroni NJ. Biology of *Pseudomonas stutzeri*. Microbiol. Mol. Biol. Rev. 2006;70(2):510–547. doi:10.1128/MMBR.00047-05.

Lesser MP, Falcon LI, Rodriguez-Roman A, Enriquez S, Hoegh-Guldberg O, Iglesias-Prieto R. Nitrogen fixation by symbiotic cyanobacteria provides a source of nitrogen for the scleractinian coral *Montastraea cavernosa*. Mar. Ecol. Prog. Ser. 2007;346:143–52. doi: 10.3354/meps07008.

Li J, Long L, Zou Y, Zhang S. Microbial community and transcriptional responses to increased temperatures in coral *Pocillopora damicornis* holobiont. Environ. Microbiol. 2021;23(2):826–43. doi: 10.1111/1462-2920.15168.

Littman R, Willis BL, Bourne DG. Metagenomic analysis of the coral holobiont during a natural bleaching event on the Great Barrier Reef. Environ. Microbiol. Rep. 2011;3(6):651–60. doi: 10.1111/j.1758-2229.2010.00234.x.

Lyndby NH, Holm JB, Wangpraseurt D, Grover R, Rottier C, Kuhl M et al. Effect of temperature and feeding on carbon budgets and O2 dynamics in *Pocillopora damicornis*. Mar. Ecol. Prog. Ser. 2020;652:49–62. doi: 10.3354/meps13474.

Martino C, Morton J, Marotz C, Thompson L, Tripathi A, Knight R et al. A novel sparse compositional technique reveals microbial perturbations. mSystems. 2019;4:1–13. doi: 10.1128/mSystems.00016-19.

1015 Matsuda S, Huffmyer A, Lenz E, Davidson J, Hancock J, Przybylowski et al. Coral Bleaching
1016 Susceptibility Is Predictive of Subsequent Mortality Within but Not Between Coral Species.
1017 Front. Ecol. Evol. 2020;8. doi: 10.3389/fevo.2020.00178.
1018 Matsuda S. The effects of ocean warming on coral symbioses: algal symbiosis establishment,
1019 bleaching and recovery. Doctoral dissertation. University of Hawai'i (USA)2021;pp234.
1020 https://scholarspace.manoa.hawaii.edu/server/api/core/bitstreams/431a138a-d7ba-4f10-
1021 bef0-7c6aa938a4cd/content.
1022 McDevitt-Irwin JM, Baum JK, Garren M, Vega Thurber R. Responses of coral-associated
1023 abcterial communities to local and global stressors. Front. Mar. Sci. 2017;4. doi:
1024 10.3389/fmars.2017.00262.
1025 McGee KM, Eaton WD, Shokralla S, Hajibabaei M. Determinants of soil bacterial and fungal
1026 community composition toward carbon-use efficiency across primary and secondary forests
1027 in a costa rican conservation area. Microb. Ecol. 2019;77(1):148–67. doi: 10.1007/s00248-
1028 018-1206-0.
1029 McGinley MP, Aschaffenburg MD, Pettay DT, Smith RT, LaJeunesse TC, Warner ME.
1030 *Symbiodinium* spp. in colonies of eastern Pacific *Pocillopora* spp. are highly stable despite
1031 the prevalence of low-abundance background populations. Mar. Ecol. Prog. Ser.
1032 2012;462:1–7. doi: 10.3354/meps09914.
1033 Meunier V, Bonnet S, Pernice M, Benavides M, Lorrain A, Grosso O et al. Bleaching forces
1034 coral's heterotrophy on diazotrophs and *Synechococcus*. ISME J. 2019;13:2882–6. doi:
1035 10.1038/s41396-019-0456-2.
1036 Morton JT, Marotz C, Washburne A, Silverman J, Zaramela LS, Edlund A, et al. Establishing
1037 microbial composition measurement standards with reference frames. Nat. Commun.
1038 2019;10:1–11. doi: 10.1038/s41467-019-10656-5.
1039 Neave MJ, Michell CT, Apprill A, Voolstra CR. *Endozoicomonas* genomes reveal functional
1040 adaptation and plasticity in bacterial strains symbiotically associated with diverse marine
1041 hosts. Sci. Rep. 2017;7:40579. doi: 10.1038/srep40579.

1042 Neave, MJ, Apprill A, Ferrier-Pagès C, Voolstra CR. Diversity and function of prevalent
1043 symbiotic marine bacteria in the genus *Endozoicomonas*. Appl. Microbiol. Biotechnol.
1044 2016;100:8315–24. doi: 10.1007/s00253-016-7777-0.
1045 O'Dea, A, Lepore M, Altieri AH, Chan M, Morales-Saldaña JM, Muñoz NH et al. Defining
1046 variation in pre-human ecosystems can guide conservation: An example from a Caribbean
1047 coral reef. Sci. Rep. 2020;10:2922. doi: 10.1038/s41598-020-59436-y.
1048 Olson ND, Ainsworth TD, Gates RD, Takabayashi M. Diazotrophic bacteria associated with
1049 Hawaiian *Montipora* corals: diversity and abundance in correlation with symbiotic
1050 dinoflagellates. J. Exp. Mar. Biol. Ecol. 2009;371:140–6. doi: 10.1016/j.jembe.2009.01.012.
1051 Osman EO, Suggett DJ, Voolstra CR, Pettay DT, Clark DR, Pogoreutz C et al. Coral
1052 microbiome composition along the northern Red Sea suggests high plasticity of bacterial
1053 and specificity of endosymbiotic dinoflagellate communities. Microbiome. 2020;8:1–16.
1054 doi: 10.1186/s40168-019-0776-5.
1055 Parada AE, Needham DM, Fuhrman JA. Every base matters: assessing small subunit rRNA
1056 primers for marine microbiomes with mock communities, time series and global field
1057 samples. Environ. Microbiol. 2016;18(5):1403–14. doi: 10.1111/1462-2920.13023.
1058 Pauvert C, Buée M, Laval V, Edel-Hermann V, Fauchery L, Gautier A, et al. Bioinformatics
1059 matters: The accuracy of plant and soil fungal community data is highly dependent on the
1060 metabarcoding pipeline. Fungal Ecol. 2019;41:23–33. doi: 10.1016/j.funeco.2019.03.005.
1061 Peixoto RS, Rosado PM, Leite DCA, Rosado AS, Bourne DG. Beneficial microorganisms for
1062 corals (BMC): proposed mechanisms for coral health and resilience. Front. Microbiol.
1063 2017;8:341. doi: 10.3389/fmicb.2017.00341.
1064 Pogoreutz C, Rädecker N, Cárdenas A, Gärdes A, Wild C, Voolstra CR. Dominance of
1065 *Endozoicomonas* bacteria throughout coral bleaching and mortality suggests structural
1066 inflexibility of the *Pocillopora verrucosa* microbiome. Ecol. Evol. 2018;8:2240–52. doi:
1067 10.1002/ece3.3830.

1068 Putnam HM, Gates RD. Preconditioning in the reef building coral *Pocillopora damicornis* and
1069 the potential for trans-generational acclimatization in coral larvae under future climate
1070 change conditions. J. Exp. Biol. 2015;218:2365–72. doi 10.1242/jeb.123018.
1071 Quast C, Pruesse E, Yilmaz P, Gerken J, Schweer T, Yarza P, et al. The SILVA ribosomal RNA
1072 gene database project: improved data processing and web-based tools. Nucleic Acids Res.
1073 2013;41:590–6. doi: 10.1093/nar/gks1219.
1074 R Core Team. R: a language and environment for statistical computing. R Found. Stat. Comput.
1075 2014. http://www.r-project.org.
1076 Raina JB, Dinsdale EA, Willis BL, Bourne DG. Do the organic sulfur compounds DMSP and
1077 DMS drive coral microbial associations? Trends Microbiol. 2010;18(3):101–8. doi:
1078 10.1016/j.tim.2009.12.002.
1079 Ravindran J, Kannapiran E, Manikandan B, Francis K, Shruti A, Karunya E et al. UV-absorbing
1080 bacteria in coral mucus and their response to simulated temperature elevations. Coral Reefs.
1081 2013;32:1043–50. doi: 10.1007/s00338-013-1053-x.
1082 Ritson-Williams R, Gates RD. Coral community resilience to successive years of bleaching in
1083 Kāne‘ohe Bay, Hawai‘i. Coral Reefs. 2020;39. doi: 10.1007/s00338-020-01944-4.
1084 Rivers AR, Weber KC, Gardner TG, Liu S, Armstrong SD. ITSxpress: software to rapidly trim
1085 internally transcribed spacer sequences with quality scores for marker gene analysis.
1086 F1000Res. 2018;7:1418. doi: 10.12688/f1000research.15704.1.
1087 Rouzé H, Lecellier G, Pochon X, Torda G, Berteaux-Lecellier V. Unique quantitative
1088 Symbiodiniaceae signature of coral colonies revealed through spatio-temporal survey in
1089 Moorea. Sci. Rep. 2019;9:7921. doi: 10.1038/s41598-019-44017-5.
1090 Rowan R, Knowlton N, Baker A, Jara J. Landscape ecology of algal symbionts creates variation
1091 in episodes of coral bleaching. Nature. 1997;388:265–9. doi: 10.1038/40843.
1092 Rowan R, Powers DA. A molecular genetic classification of zooxanthellae and the evolution of
1093 animal-algal symbioses. Science. 1991;15:251(4999):1348–51. doi:
1094 10.1126/science.251.4999.1348.

1095 Salerno JL, Reineman DR, Gates RD, Rappé MS. The effect of a sublethal temperature
1096 elevation on the structure of bacterial communities associated with the coral *Porites*
1097 *compressa*. J. Mar. Biol. 2010;2011:1–9. doi: 10.1155/2011/969173.
1098 Sampayo EM, Ridgway TM, Bongaerts P, Hoegh-Guldberg O. Bleaching susceptibility and
1099 mortality of corals are determined by fine-scale differences in symbiont type. Proc. Nat.
1100 Acad. Sci. 2008;105:10444–9. doi: 10.1073/pnas.0708049105.
1101 Santos HF, Carmo FL, Duarte G, Dini-Andreote F, Castro CB, Rosado AS, et al. Climate
1102 change affects key nitrogen-fixing bacterial populations on coral reefs. ISME J.
1103 2008;8:2272–9. doi: 10.1038/ismej.2014.70.
1104 Shaffer M. SCNIC: sparse cooccurrence network investigation for compositional data. 2020.
1105 https://github.com/shafferm/SCNIC.
1106 Shannon P, Markiel A, Ozier O, Baliga NS, Wang JT, Ramage D et al. Cytoscape: a software
1107 environment for integrated models of biomolecular interaction networks Genome Res.
1108 2003;13(11):2498–504. doi: 10.1101/gr.1239303.
1109 Shore-Maggio A, Runyon CM, Ushijima B, Aeby GS, Callahan SM. Differences in bacterial
1110 community structure in two color morphs of the Hawaiian reef coral *Montipora capitata*.
1111 Appl. Environ. Microbiol. 2015;81:7312–8. doi: 10.1128/AEM.01935-15.
1112 Silverstein RN, Cunning R, Baker AC. Change in algal symbiont communities after bleaching
1113 not prior heat exposure, increases heat tolerance of reef corals. Glob. Change Biol.
1114 2015;21:236–49. doi: 10.1111/gcb.12706.
1115 Sinha RP, Klisch M, Helbling EW, Hader DP. Induction of mycosporine—like amino acids
1116 (MAAs) in cyanobacteria by solar ultraviolet-B radiation. J. Photochem. Photobiol. B.
1117 2001;60:129–35. doi: 10.1016/s1011-1344(01)00137-3.
1118 Smith H, Epstein H, Torda G. The molecular basis of differential morphology and bleaching
1119 thresholds in two morphs of the coral *Pocillopora acuta*. Sci. Rep. 2017;7:1–12. doi:
1120 10.1038/s41598-017-10560-2.
1121 Speck M, Donachie SP. Widespread Oceanospirillaceae Bacteria in *Porites* spp. J. Mar. Biol.
1122 2012;1–7. doi:10.1155/2012/746720.

Stat M, Loh WKW, LaJeunesse TC, Hoegh-Guldberg O, Carter DA. Stability of coral–endosymbiont associations during and after a thermal stress event in the southern Great Barrier Reef. Coral Reefs. 2009;28:709–713. doi: 10.1007/s00338-009-0509-5.

Stat M, Pochon X, Franklin EC, Bruno JF, Casey KS, Selig ER et al. The distribution of the thermally tolerant symbiont lineage (*Symbiodinium* clade D) in corals from Hawaii: correlations with host and the history of ocean thermal stress. Ecol. Evol. 2013;3(5):1317–29. doi:10.1002/ece3.556

Tout J, Siboni N, Messer LF, et al. Increased seawater temperature increases the abundance and alters the structure of natural *Vibrio* populations associated with the coral *Pocillopora damicornis*. Front. Microbiol. 2015;6:432 doi: 10.3389/fmicb.2015.00432.

Turnham KE, Wham DC, Sampayo E, LaJeunesse TC. Mutualistic microalgae co-diversify with reef corals that acquire symbionts during egg development. ISME J. 2021;15(11):3271–85. doi: 10.1038/s41396-021-01007-8.

Van Oppen MJH, Medina M. Coral evolutionary responses to microbial symbioses. Philos. Trans. R. Soc. Lond. B. 2020;375:20190591. doi: 10.1098/rstb.2019.0591.

Vega Thurber R, Willner-Hall D, Rodriguez-Mueller B, Desnues C, Edwards RA, Angly F et al. Metagenomic analysis of stressed coral holobionts. Environ. Microbiol. 2009;11(8):2148–63. doi: 10.1111/j.1462-2920.2009.01935.x.

Wall C, Ritson-Williams R, Popp B, Gates R. Spatial variation in the biochemical and isotopic composition of corals during bleaching and recovery. Limnol. Oceanogr. 2019;64(5):2011–28. doi: 10.1002/lno.11166.

Wham DC, Ning G, LaJeunesse TC. Data from: *Symbiodinium glynnii* sp. nov., a species of stress-tolerant symbiotic dinoflagellates from pocilloporid and montiporid corals in the Pacific Ocean, Dryad, Dataset 2017. doi: 10.5061/dryad.mg363.

Yilmaz P, Parfrey LW, Yarza P, Gerken J, Pruesse E, Quast C, et al. The SILVA and "all-species Living Tree Project (LTP)" taxonomic frameworks. Nucleic Acids Res. 2014;42:643–8. doi: 10.1093/nar/gkt1209.

Zhou G, Tong H, Cai L, Huang H. Transgenerational effects on the coral *Pocillopora damicornis* microbiome under ocean acidification. Microb. Ecol. 2021;82(3):572–80. doi: 10.1007/s00248-021-01690-2.

Ziegler M, Grupstra CG, Barreto MM, Eaton M, BaOmar J, Zubier K et al. Coral bacterial community structure responds to environmental change in a host-specific manner. Nat. Commun. 2019;10:3092. doi: 10.1038/s41467-019-10969-5.

Ziegler M, Roik A, Porter A, Zubier K, Mudarris MS, Ormond R et al. Coral microbial community dynamics in response to anthropogenic impacts near a major city in the central Red Sea. Mar. Pollut. Bull. 2016;105:629–40. doi: 10.1016/j. marpolbul.2015.12.045.

Ziegler M, Seneca F, Yum L, Garren M, Stocker R, Webster NS et al. Bacterial community dynamics are linked to patterns of coral heat tolerance. Nat. Commun. 2017;8:14213. doi: 10.1038/ncomms14213.

Figure legends

Fig. 1. Map of Kane'ohe (O'ahu) in the Hawai'ian archipelago. Experimental coral sampling scheme from tagged corals in the field, where 1.5 cm fragments were collected for each colony in all sample groups (n = 10): Mcap_B, Mcap_NB, Pcom_B, Pcom_NB, and Pacu _B on five occasions during the recovery after the first beaching event: M0: Oct 2014; M1: Nov 2014; M3: Jan 2015, M6: May 2015, M12: Sept 2015. Species: Mcap: *Montipora capitata*, Pcom:s *Porites compressa*, Pacu: *Pocillopora acuta*. Bleaching susceptibility: B: susceptible colonies; NB: resistant colonies.

Fig. 2. Prokaryotic composition at the genus level (> 0.1 % detection) for the three coral species. Bars are collapsed by species, month after bleaching event and bleaching susceptibility phenotypes; and grouped for species and bleaching susceptibility. Species: Mcap: *Montipora capitata*, Pcom:s *Porites compressa*, Pacu: *Pocillopora acuta*. Bleaching susceptibility: B: susceptible colonies; NB: resistant colonies. Month after bleaching event: M0: Oct 2014; M1: Nov 2014; M3: Jan 2015, M6: May 2015, M12: Aug 2015 (Table S1).

Fig. 3. Volatility of the log-ratios of the microbial/bacterial balance representing the differential taxa across time for the three coral species, by bleaching susceptibility phenotypes. **A)** *Montipora capitata*; **B)** *Pocillopora acuta*; and **C)** *Porites compressa* corals. Numerator and denominator taxa forming each balance are shown in each plot grouped at the genus level, or the next lowest taxonomic annotation. *Represents time points with significant dissimilarities between B and NB colonies (Welch tests $p < 0.05$). §Indicates significant divergence on log-ratio longitudinally over time (LME; $P>[z] < 0.05$). **D)** Trajectory plots over time of differentially abundant bacterial taxa at the ASV level for the three coral species, by bleaching susceptibility phenotypes. Taxa are named by the lowest taxonomical annotation. Double dashed lines represent selected numerator taxa, while single dashed lines represent denominator taxa within each coral subset. Mcap: *Montipora capitata*, Pcom *Porites compressa*, Pacu: *Pocillopora acuta*; NB: Bleaching resistant colonies, B: Bleaching susceptible colonies;

Months after the bleaching event: M0: Oct 2014; M1: Nov 2014; M3: Jan 2015, M6: May 2015, M12: Sept 2015.

Fig. 4. Symbiodiniaceae community composition of the three coral species across time points – 0 (M0), 1 (M1), 3 (M3) and 6 (M6) months after the bleaching event, and beaching susceptibility phenotypes –Bleaching susceptible (B) and resistant (NB) colonies. Each column represents a coral fragment/sample at each collection point. Microalgal IDs are depicted by the relative abundance of ITS2 sequences (> 3 % detection) plotted in the upper bars, and predicted ITS2 profiles plotted in the bars below (normalized to 1). **A)** *Montipora capitata* (Mcap); **B)** *Porites compressa* (Pcom) ; **C)** *Pocillopora acuta* (Pacu).

Fig. 5. Volatility of the log-ratios of the balance formed by the ITS2 sequences representing the top differential phylotypes in two coral species by bleaching susceptibility phenotypes across time. **A)** *Montipora capitata*: The balance included 23 top ranked numerator DIVs comprising some C31, C17 and C21 and other C DIVs; and 23 top ranked denominator DIVs, formed by D4, D1, D6, D1ab and D3h, and a few C17 and C21 among other C DIVs. **B)** *Porites compressa*: In the balance 12 top ranked numerator DIVs included C3 and other C DIVs; and the 12 top ranked denominator DIVs comprised several C15 and other C DIVs. *Represents time points with significant dissimilarities between B and NB colonies (Welch tests $p < 0.05$). RPCA compositional biplot based on Aitchison distances (DEICODE) of the total Symbiodiniaceae ITS2 sequences from coral fragments belonging to two species at four time points –0 (M0), 1 (M1), 3 (M3) and 6 (M6) months after the bleaching event. Samples (circles) were distinguished by colour according to Bleaching susceptibility. **C)** *Montipora capitata* (Mcap) showed differences in B *vs* NB colonies at M0, M1 and M3. **D)** *Porites compressa* (Pcom) revealed divergencies in B *vs* NB colonies only at t0 (PERMANOVA, $p < 0.05$). Ten most relevant DIVs driving differences in the ordination space are illustrated by the vectors in each plot.

Fig. 6. Cross co-occurrence networks of bacteria phylotypes at the ASV level *vs* ITS2 type profiles built on SCNIC for the three coral species, by bleaching susceptibility phenotypes 0 (Oct 2014 –M0), 1 (Nov 2014 –M1), 3 (Jan 2015 –M3) and 6 (May 2015 –M6) months after the bleaching event. Mcap: *Montipora capitata*, Pcom *Porites compressa*, Pacu: *Pocillopora acuta*; B: Bleaching susceptible colonies, NB: Bleaching resistant colonies. In the networks bacterial ASVs are represented by pink hexagons, Symbiodiniaceae type profiles of the *Cladocopium* clade are green circles and *Durusdinium* are orange circles. Negative interactions are depicted by red arrows and quantified as red numbers / positive interactions by green arrows and green numbers.

Kane'ohe Bay, Oahu (Hawai'i)

Coral bleaching Oct 2014

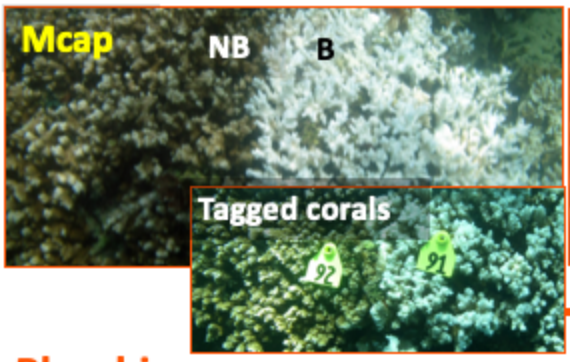

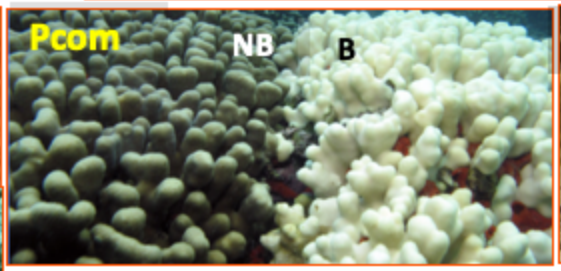

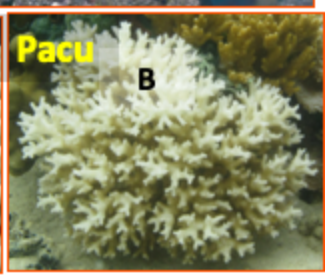

n = 10

Bleaching → Recovery → Pre-bleaching

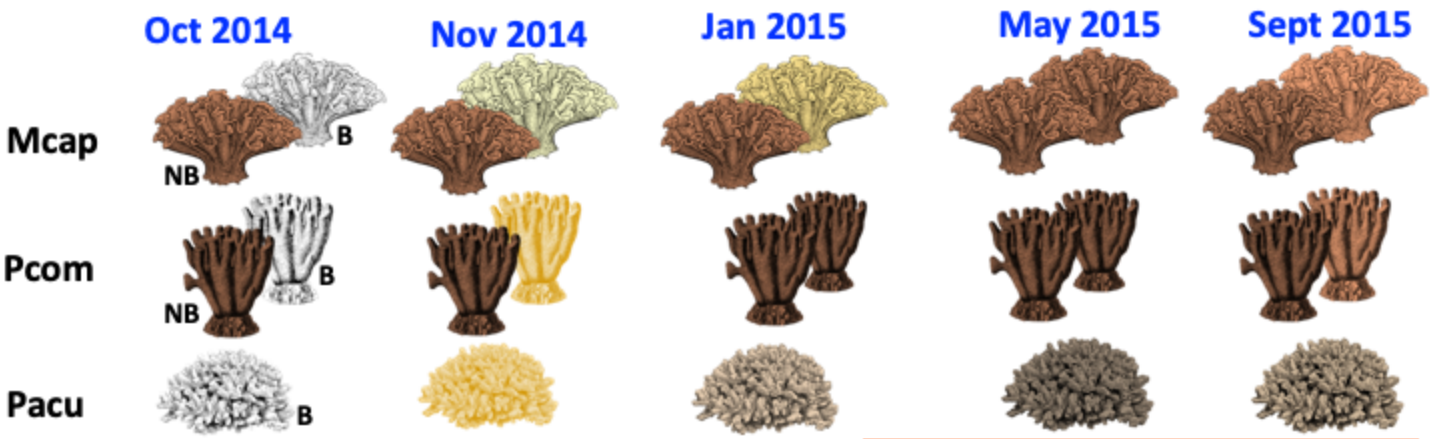

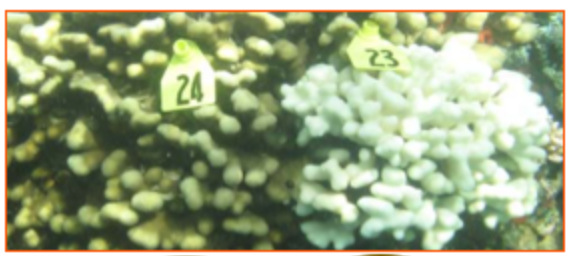

Coral microbiomes

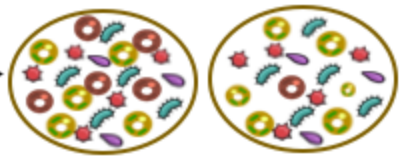

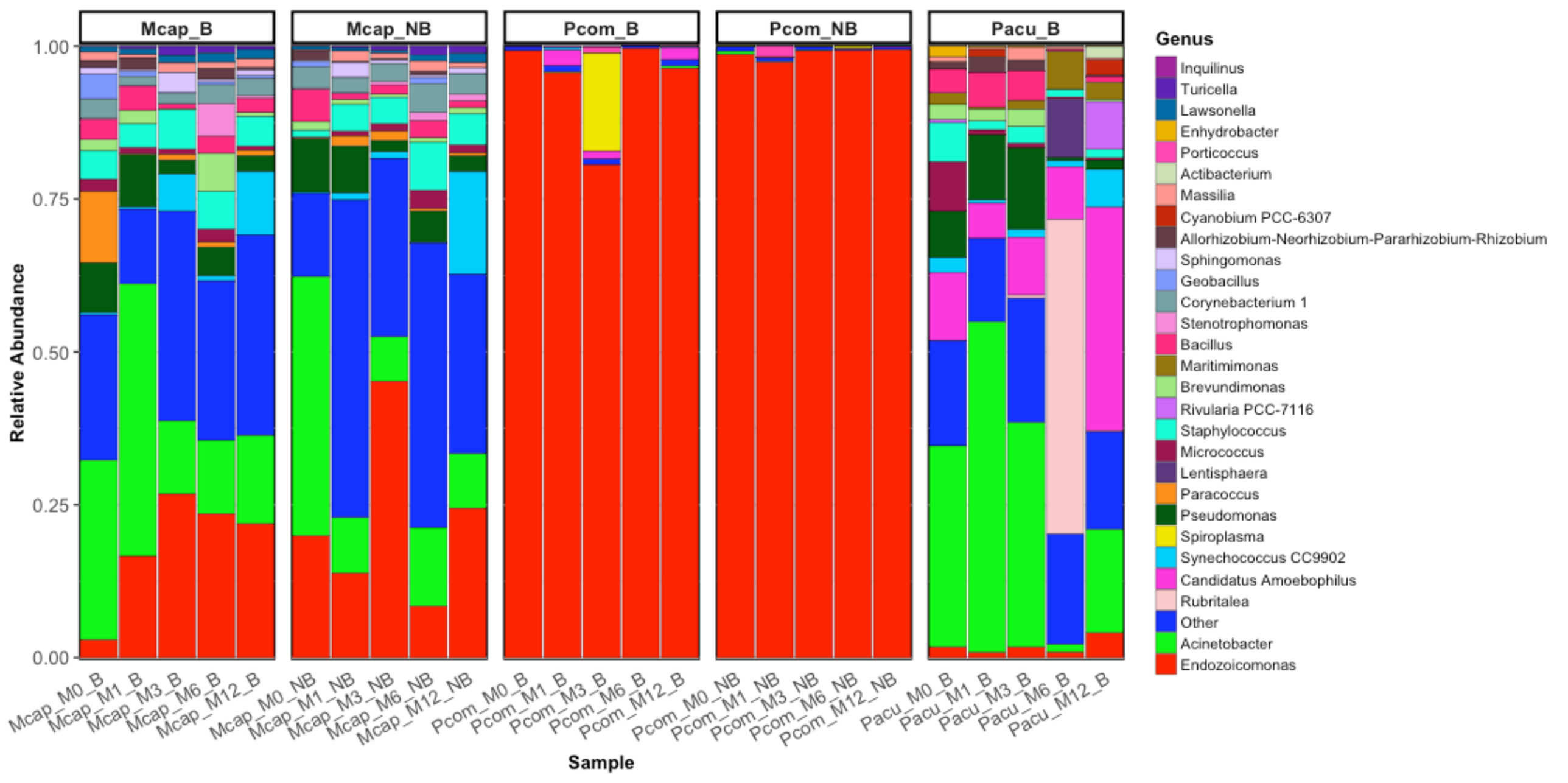
Mcap_B
Mcap_NB
Pcom_B
Pcom_NB
Pacu_B
Relative Abundance
1.00
0.75
0.50
0.25
0.00
Mcap_M0_B
Mcap_M1_B
Mcap_M3_B
Mcap_M6_B
Mcap_M12_B
Mcap_M0_NB
Mcap_M1_NB
Mcap_M3_NB
Mcap_M6_NB
Mcap_M12_NB
Pcom_M0_B
Pcom_M1_B
Pcom_M3_B
Pcom_M6_B
Pcom_M12_B
Pcom_M0_NB
Pcom_M1_NB
Pcom_M3_NB
Pcom_M6_NB
Pcom_M12_NB
Pacu_M0_B
Pacu_M1_B
Pacu_M3_B
Pacu_M6_B
Pacu_M12_B
Sample
Genus
Inquilinus
Turicella
Lawsonella
Enhydrobacter
Porticoccus
Actibacterium
Massilia
Cyanobium PCC-6307
Allorhizobium-Neorhizobium-Pararhizobium-Rhizobium
Sphingomonas
Geobacillus
Corynebacterium 1
Stenotrophomonas
Bacillus
Maritimimonas
Brevundimonas
Rivularia PCC-7116
Staphylococcus
Micrococcus
Lentisphaera
Paracoccus
Pseudomonas
Spiroplasma
Synechococcus CC9902
Candidatus Amoebophilus
Rubritalea
Other
Acinetobacter
Endozoicomonas

A

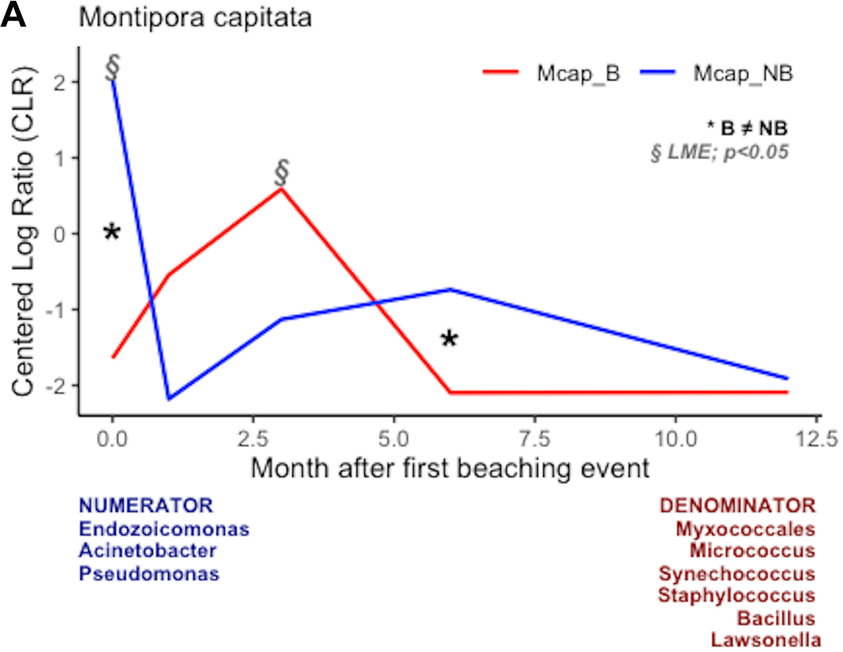
Montipora capitata
Mcap_B
Mcap_NB
* B ≠ NB
§ LME; p<0.05
Centered Log Ratio (CLR)
Month after first beaching event
NUMERATOR
Endozoicomonas
Acinetobacter
Pseudomonas
DENOMINATOR
Myxococcales
Micrococcus
Synechococcus
Staphylococcus
Bacillus
Lawsonella

B

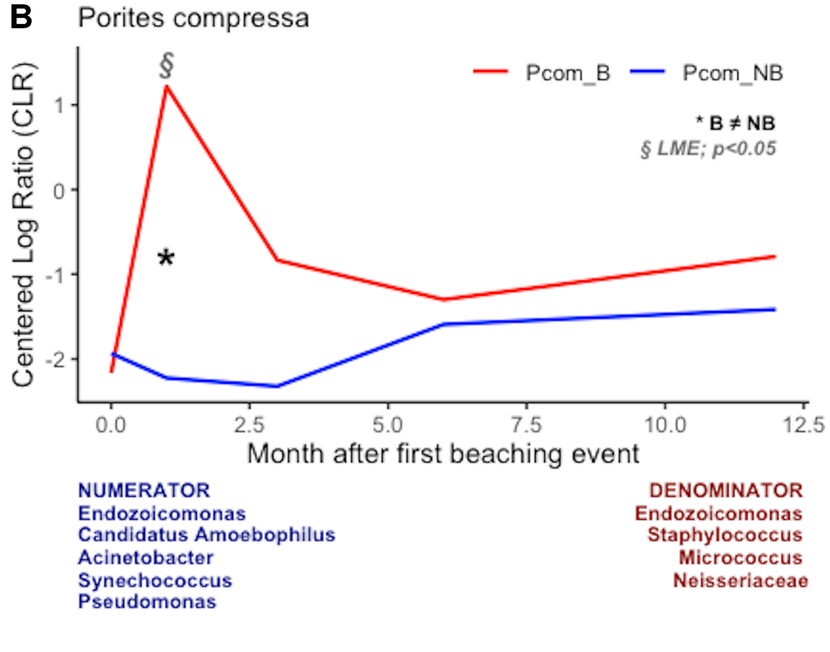
Porites compressa
Pcom_B
Pcom_NB
* B ≠ NB
§ LME; p<0.05
Centered Log Ratio (CLR)
Month after first beaching event
NUMERATOR
Endozoicomonas
Candidatus Amoebophilus
Acinetobacter
Synechococcus
Pseudomonas
DENOMINATOR
Endozoicomonas
Staphylococcus
Micrococcus
Neisseriaceae

C

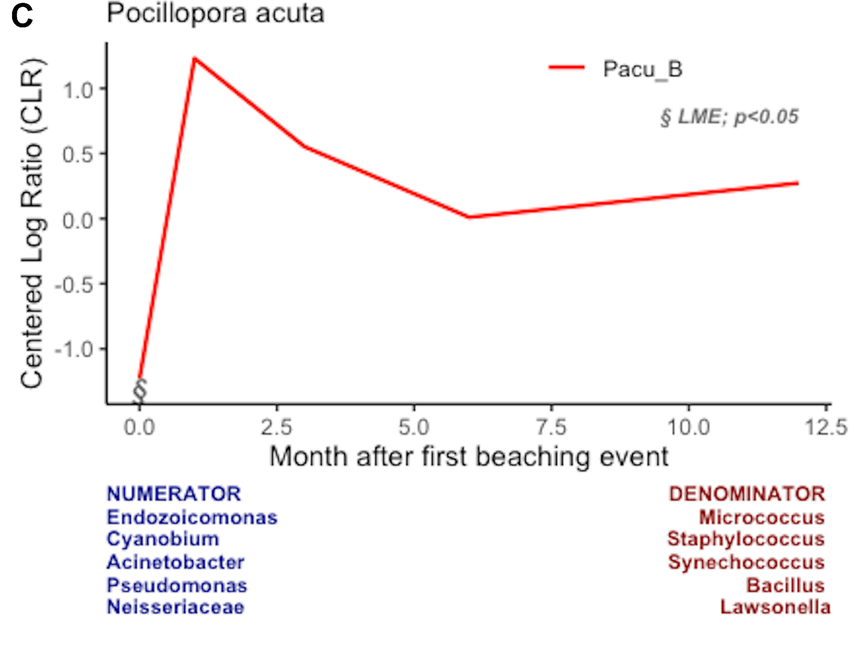
Pocillopora acuta
Pacu_B
§ LME; p<0.05
Centered Log Ratio (CLR)
Month after first beaching event
NUMERATOR
Endozoicomonas
Cyanobium
Acinetobacter
Pseudomonas
Neisseriaceae
DENOMINATOR
Micrococcus
Staphylococcus
Synechococcus
Bacillus
Lawsonella

D

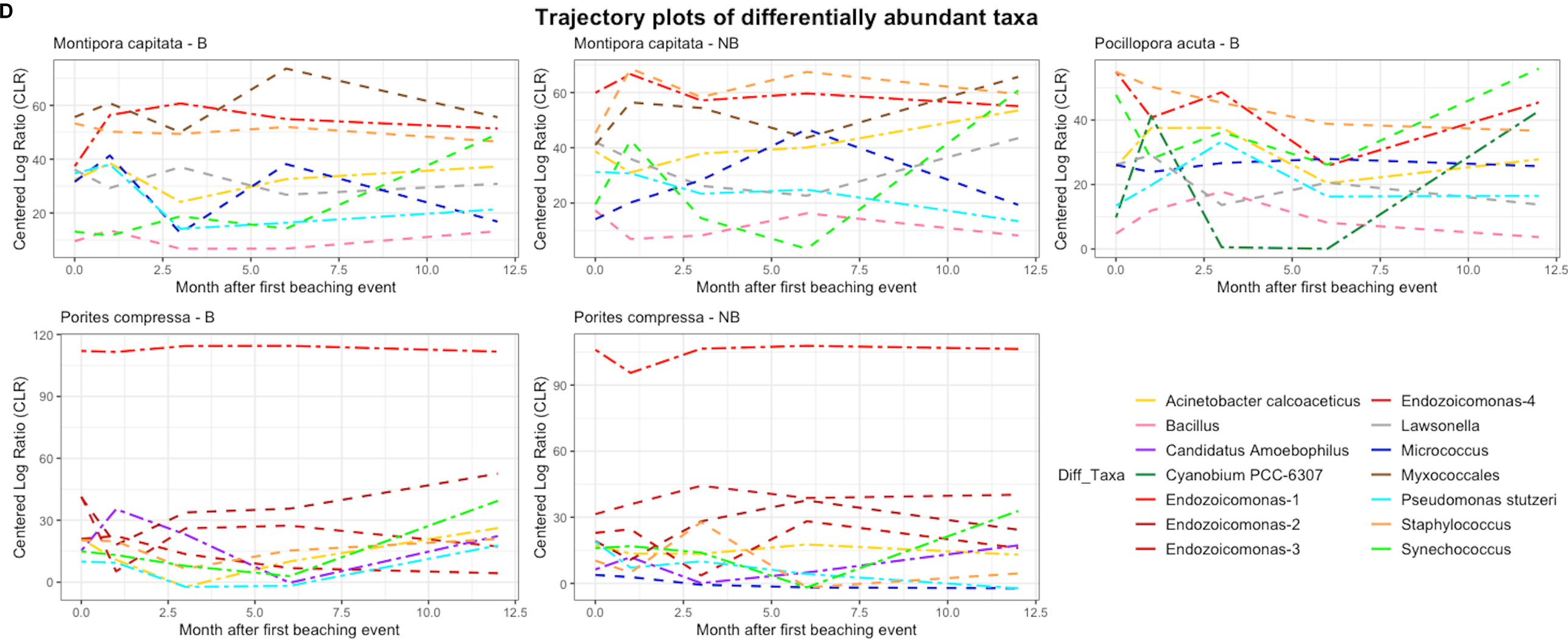
Trajectory plots of differentially abundant taxa
Montipora capitata - B
Montipora capitata - NB
Pocillopora acuta - B
Porites compressa - B
Porites compressa - NB
Centered Log Ratio (CLR)
Month after first beaching event
Diff_Taxa
Acinetobacter calcoaceticus
Bacillus
Candidatus Amoebophilus
Cyanobium PCC-6307
Endozoicomonas-1
Endozoicomonas-2
Endozoicomonas-3
Endozoicomonas-4
Lawsonella
Micrococcus
Myxococcales
Pseudomonas stutzeri
Staphylococcus
Synechococcus

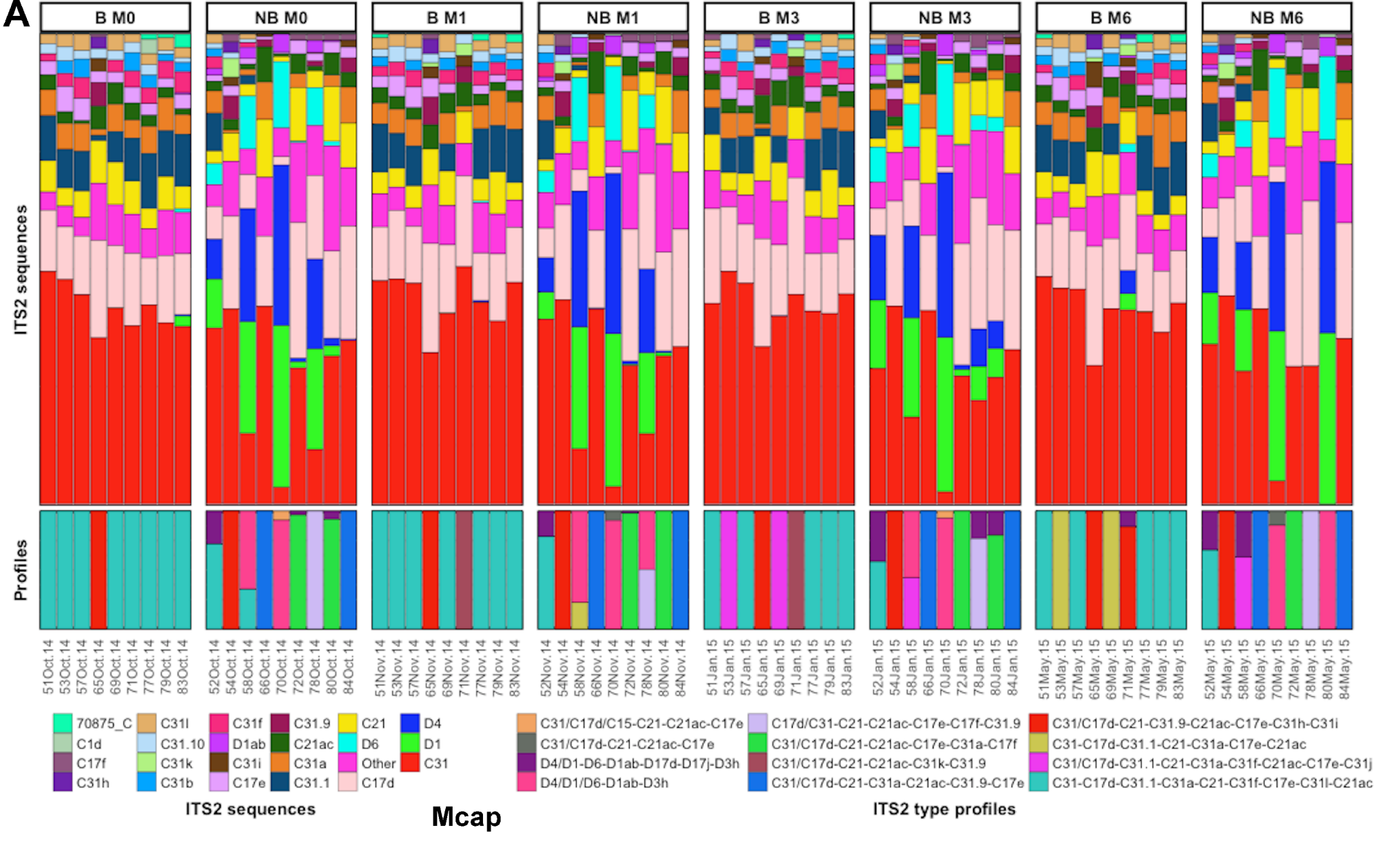
A
B M0
NB M0
B M1
NB M1
B M3
NB M3
B M6
NB M6
ITS2 sequences
Profiles
70875_C
C1d
C17f
C31h
C31l
C31.10
C31k
C31b
C31f
D1ab
C31i
C17e
C31.9
C21ac
C31a
C31.1
C21
D6
Other
C17d
D4
D1
C31
ITS2 sequences
C31/C17d/C15-C21-C21ac-C17e
C31/C17d-C21-C21ac-C17e
D4/D1-D6-D1ab-D17d-D17j-D3h
D4/D1/D6-D1ab-D3h
C17d/C31-C21-C21ac-C17e-C17f-C31.9
C31/C17d-C21-C21ac-C17e-C31a-C17f
C31/C17d-C21-C21ac-C31k-C31.9
C31/C17d-C21-C31a-C21ac-C31.9-C17e
C31/C17d-C21-C31.9-C21ac-C17e-C31h-C31i
C31-C17d-C31.1-C21-C31a-C17e-C21ac
C31/C17d-C31.1-C21-C31a-C31f-C21ac-C17e-C31j
C31-C17d-C31.1-C31a-C21-C31f-C17e-C31l-C21ac
ITS2 type profiles
Mcap

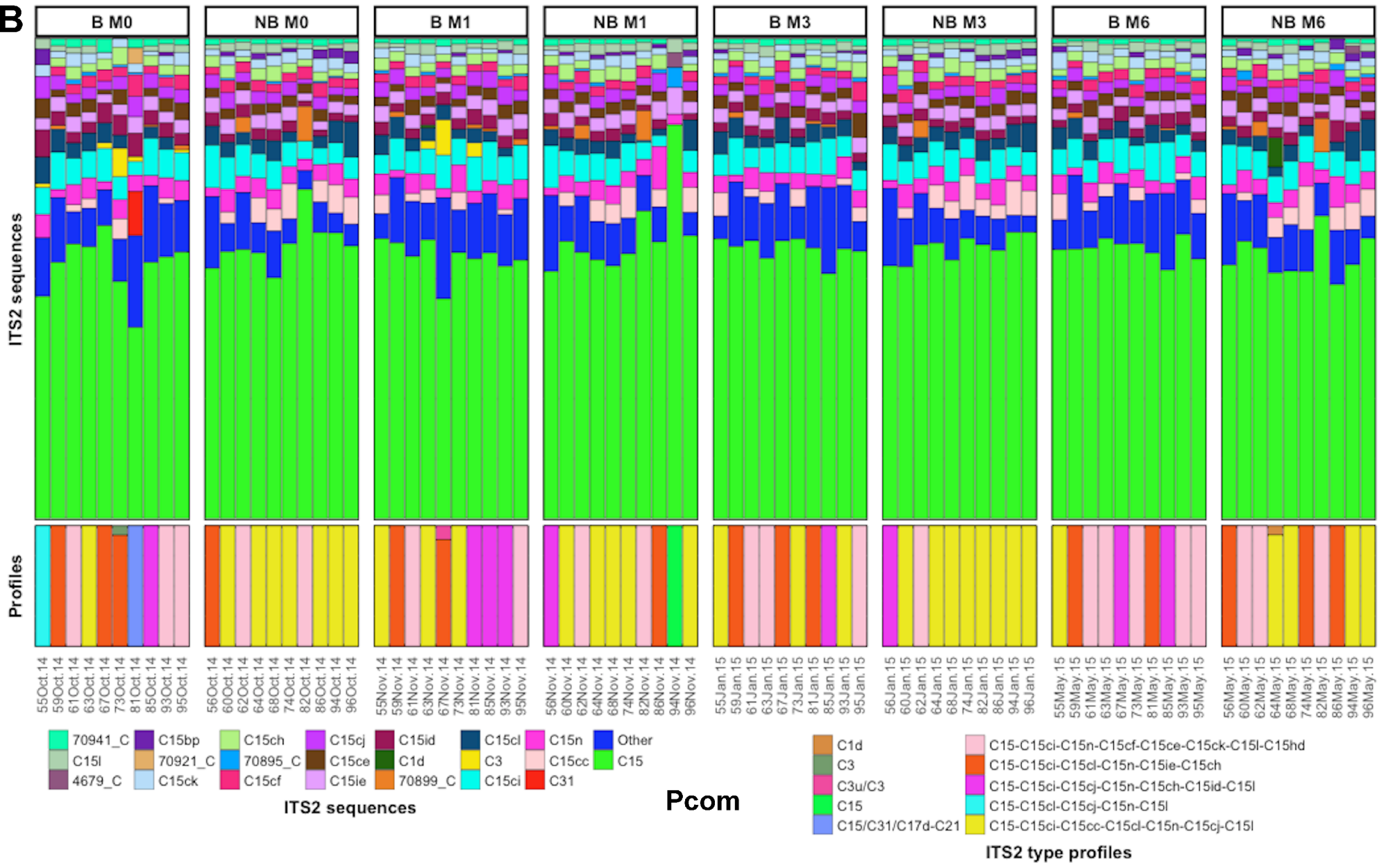
B
B M0
NB M0
B M1
NB M1
B M3
NB M3
B M6
NB M6
ITS2 sequences
Profiles
70941_C
C15l
4679_C
C15bp
70921_C
C15ck
C15ch
70895_C
C15cf
C15cj
C15ce
C15ie
C15id
C1d
70899_C
C15cl
C3
C15ci
C15n
C15cc
C31
Other
C15
ITS2 sequences
C1d
C3
C3u/C3
C15
C15/C31/C17d-C21
C15-C15ci-C15n-C15cf-C15ce-C15ck-C15l-C15hd
C15-C15ci-C15cl-C15n-C15ie-C15ch
C15-C15ci-C15cj-C15n-C15ch-C15id-C15l
C15-C15cl-C15cj-C15n-C15l
C15-C15ci-C15cc-C15cl-C15n-C15cj-C15l
ITS2 type profiles
Pcom

C
B M0
B M1
B M3
B M6
ITS2 sequences
Profiles
C15
C3cw
C1bi
C3
C1b
C3cg
Other
C1dx
C1
C42.2
C1di
C1d
C1d/C15/C1-C42.2
C1d-C1di-C42.2-C1dx-C1
C1d
C1d/C42.2/C1
C1d/C42.2/C1-C1k-C1b
C1d/C42.2-C1-C3cg
C1d-C42.2-C1-C3cg-C1b-C3cw-C115k
ITS2 sequences
ITS2 type profiles
Pacu

A

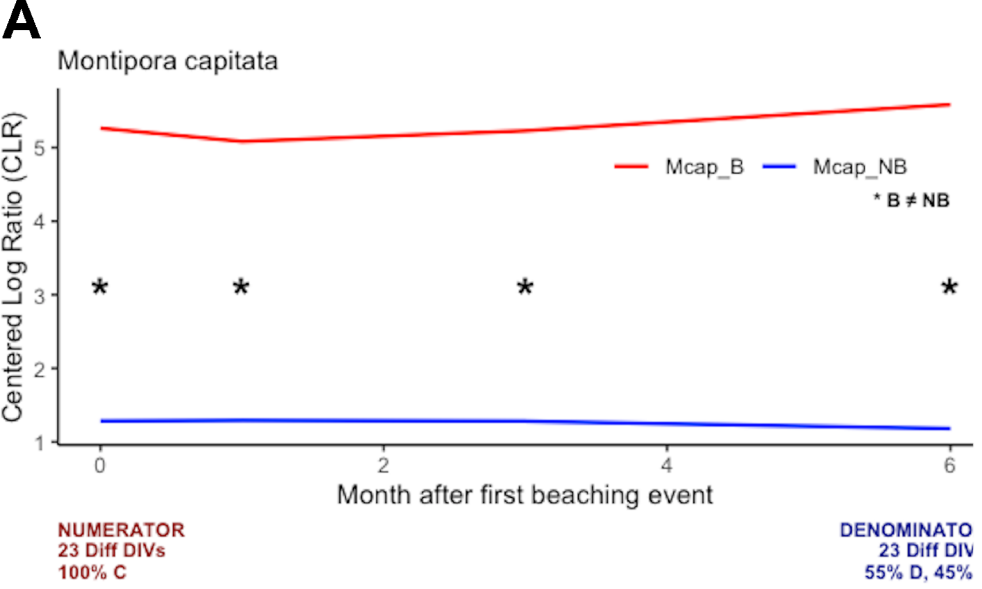
Montipora capitata
Centered Log Ratio (CLR)
Mcap_B
Mcap_NB
* B ≠ NB
Month after first beaching event
NUMERATOR
23 Diff DIVs
100% C
DENOMINATO
23 Diff DIV
55% D, 45%

B

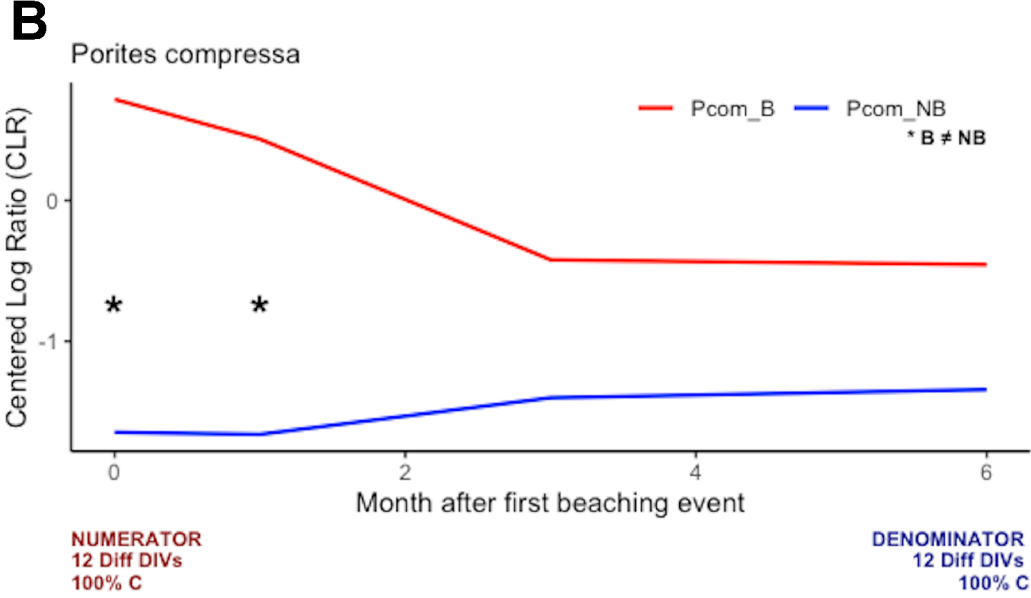
Porites compressa
Centered Log Ratio (CLR)
Pcom_B
Pcom_NB
* B ≠ NB
Month after first beaching event
NUMERATOR
12 Diff DIVs
100% C
DENOMINATOR
12 Diff DIVs
100% C

C

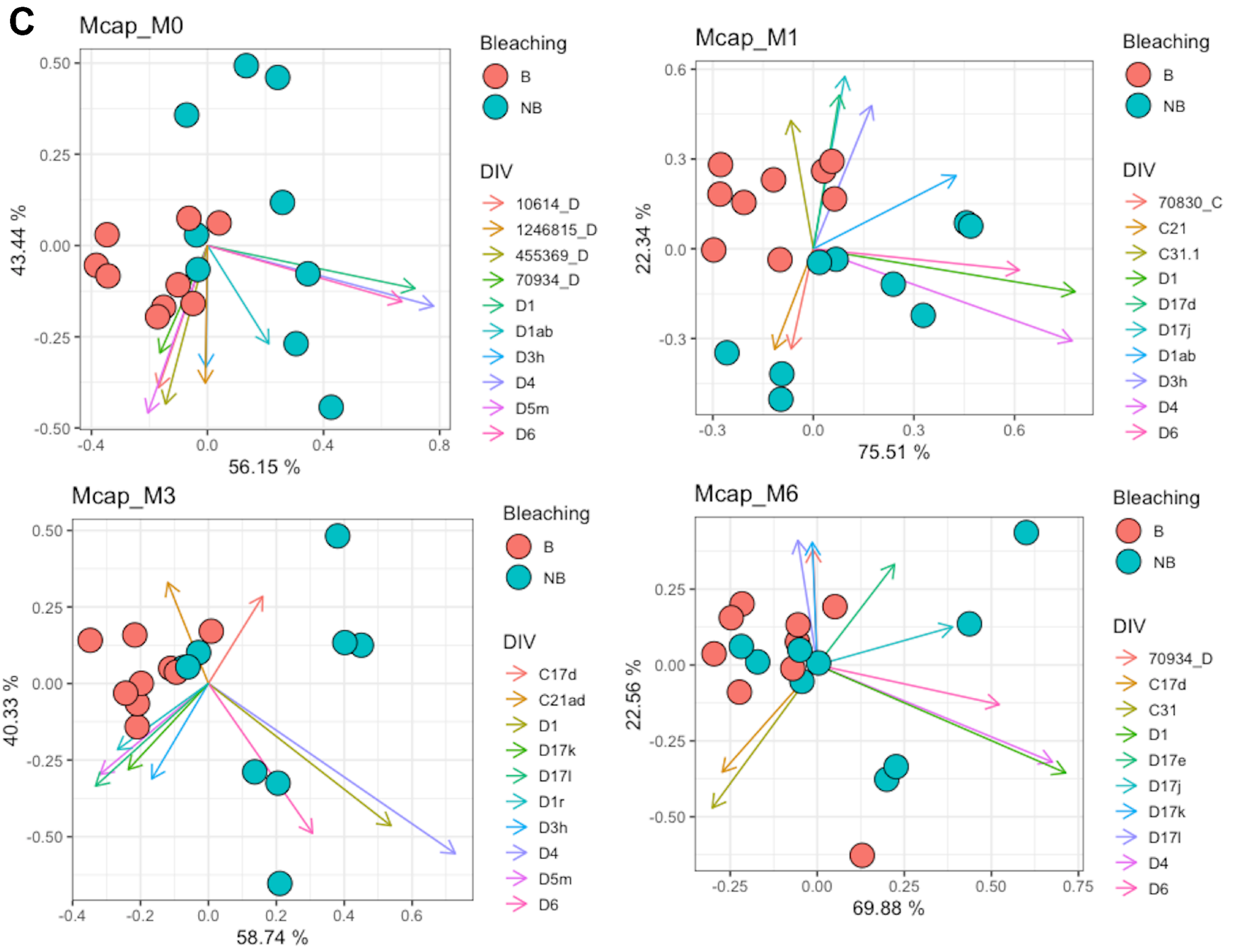
Mcap_M0
43.44 %
56.15 %
Mcap_M1
22.34 %
75.51 %
Mcap_M3
40.33 %
58.74 %
Mcap_M6
22.56 %
69.88 %
Bleaching
B
NB
DIV
10614_D
1246815_D
455369_D
70934_D
D1
D1ab
D3h
D4
D5m
D6
70830_C
C21
C31.1
D17d
D17j
C17d
C21ad
D17k
D17l
D1r
C31
D17e

D

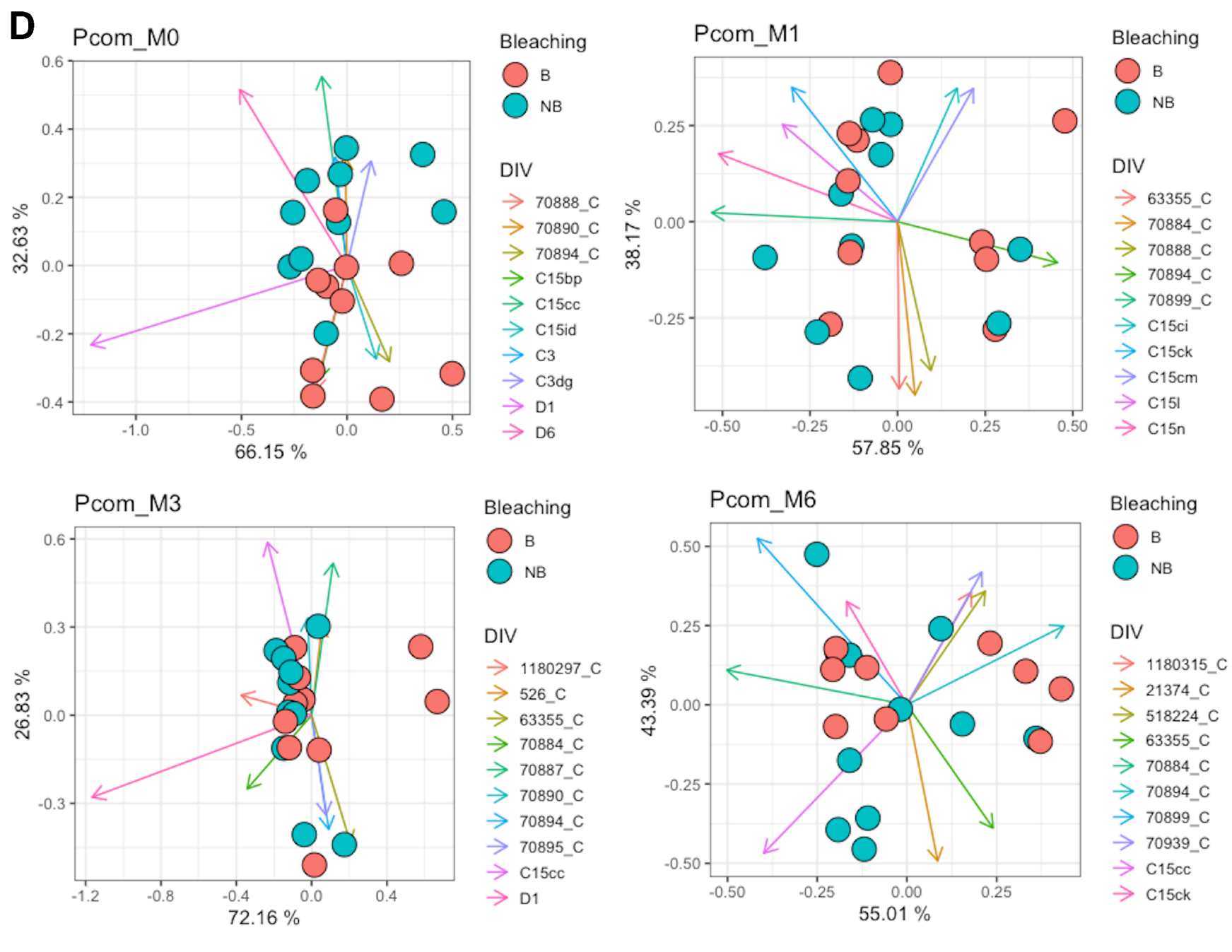
Pcom_M0
32.63 %
66.15 %
Pcom_M1
38.17 %
57.85 %
Pcom_M3
26.83 %
72.16 %
Pcom_M6
43.39 %
55.01 %
Bleaching
B
NB
DIV
70888_C
70890_C
70894_C
C15bp
C15cc
C15id
C3
C3dg
D1
D6
63355_C
70884_C
70899_C
C15ci
C15ck
C15cm
C15l
C15n
1180297_C
526_C
70887_C
70895_C
1180315_C
21374_C
518224_C

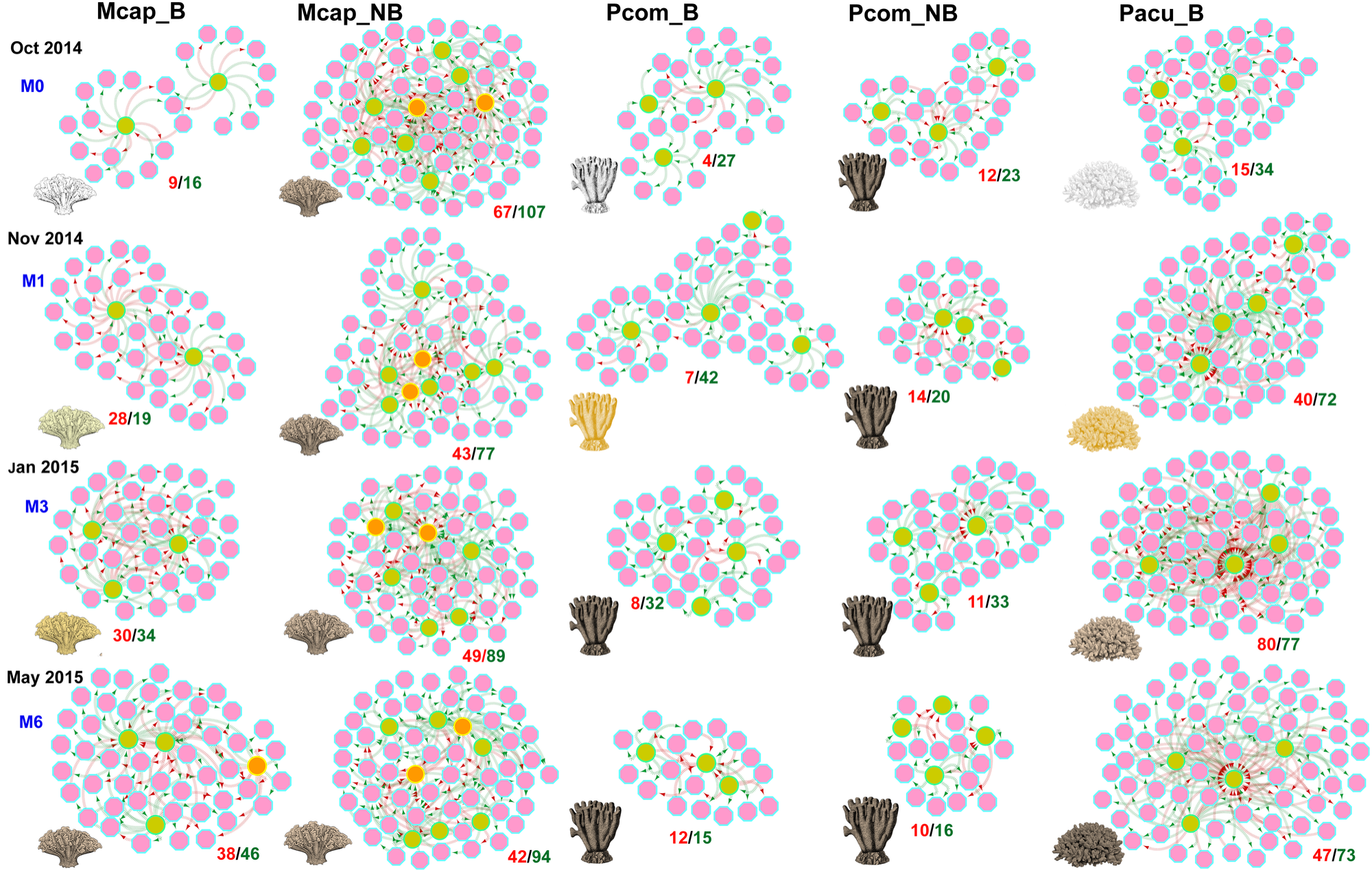
Mcap_B
Mcap_NB
Pcom_B
Pcom_NB
Pacu_B
Oct 2014
M0
9/16
67/107
4/27
12/23
15/34
Nov 2014
M1
28/19
43/77
7/42
14/20
40/72
Jan 2015
M3
30/34
49/89
8/32
11/33
80/77
May 2015
M6
38/46
42/94
12/15
10/16
47/73

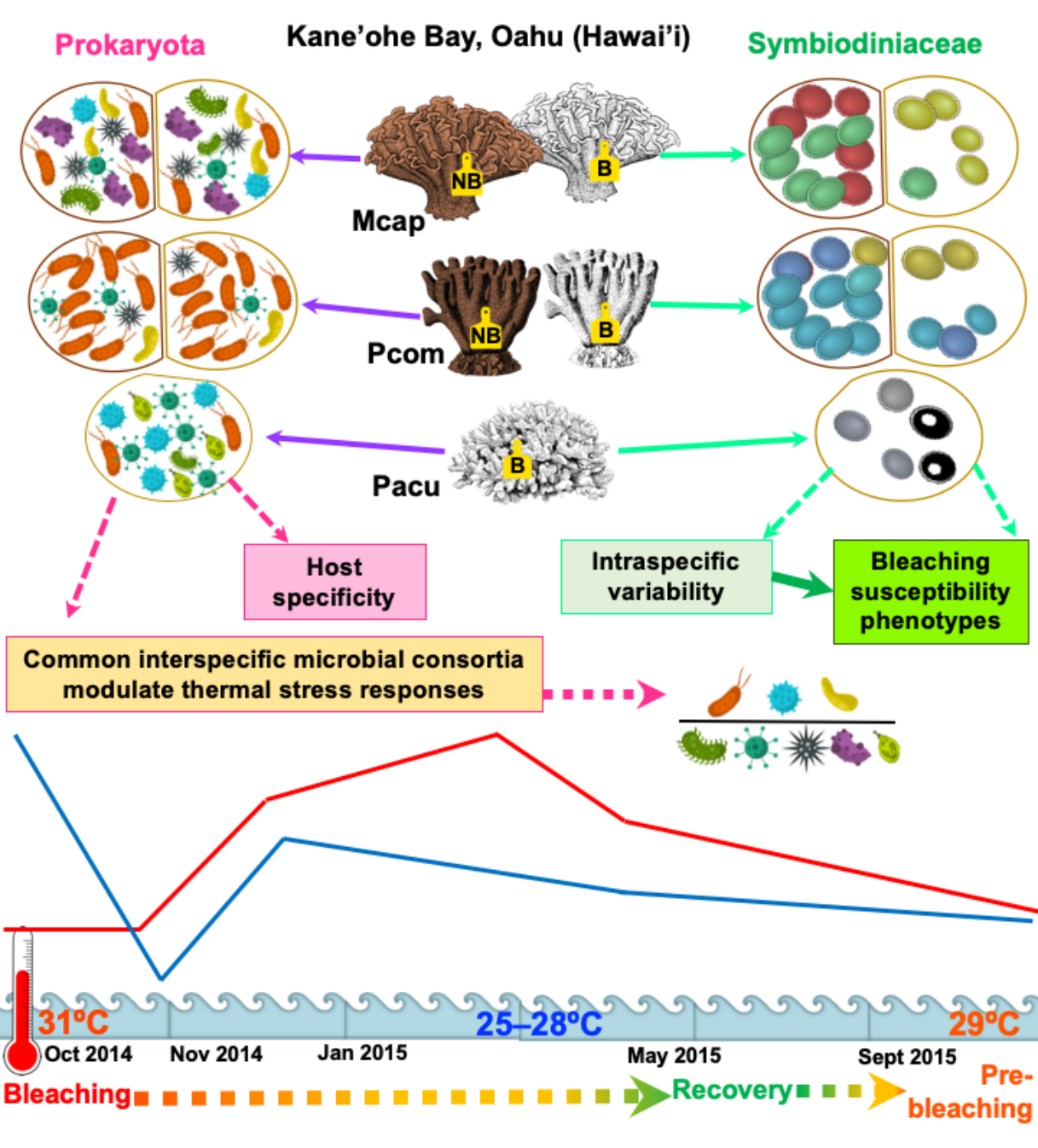
Prokaryota
Kane'ohe Bay, Oahu (Hawai'i)
Symbiodiniaceae
NB
B
Mcap
NB
B
Pcom
B
Pacu
Host specificity
Intraspecific variability
Bleaching susceptibility phenotypes
Common interspecific microbial consortia modulate thermal stress responses
31°C
25–28°C
29°C
Oct 2014
Nov 2014
Jan 2015
May 2015
Sept 2015
Bleaching
Recovery
Pre-bleaching